Metal Cation Coordination and Solvation Studied with Infrared Spectroscopy in the Gas Phase

Michael A. Duncan*

Department of Chemistry, University of Georgia, Athens, Georgia 30602, U.S.A.

*maduncan@uga.edu

Abstract

Transition metal cation-molecular complexes are produced in the gas phase environment of a molecular beam using laser ablation in a supersonic expansion. Complexes with carbon monoxide, carbon dioxide, water, acetylene, or benzene are produced by entraining small partial pressures of these molecules into an expansion of either argon or helium. A specially designed time-of-flight mass spectrometer is employed to analyze the ions produced and to mass select them for spectroscopy. Mass-selected ions are excited in the infrared region of the spectrum with a tunable IR optical parametric oscillator laser system to measure photodissociation spectroscopy in the 2000–4500 cm^{-1} region. Infrared band patterns, combined with structures and spectra predicted by density functional theory, reveal the coordination and solvation interactions in these systems, and how binding to metal distorts the structures of small molecules.

Keywords: ion-molecule complexes, mass spectrometry, ion spectroscopy, photodissociation

x.1 Introduction

Metal-molecular interactions lie at the heart of heterogeneous [1-5] and homogeneous [6,7] catalysis, metal-ligand bonding [7-11], metal ion solvation [12-14], metal chelation and sequestration [15], and the function of many biological systems [16]. Additionally, new composite materials such as metal-decorated nanotubes, metal-intercalated graphene, or metal-organic frameworks (MOFs) involve many of the same metal-molecular interactions [17-26]. These areas are critically important in petroleum processing, solar energy generation, hydrogen storage, battery materials, and related areas such as water splitting, CO_2 reduction, or heavy metal waste disposal. However, the molecular level understanding of such systems is limited because of the complexity of metal electronic structure and bonding. Conventional chemistry has documented the properties of stable metal complexes and compounds [7-11]. Likewise, heterogeneous catalysis has been studied extensively on well-characterized metal surfaces [1-3]. However, emerging catalytic systems often involve oxide-supported clusters in the ultra-small size range, with a distribution of particle sizes [4,5,27-32]. Homogeneous catalysis is mediated by metal complexes in solution with a delicate relationship between coordination and solvation [33-36]. Metal-organic and metal-carbon materials involve cation-π interactions [17-19], and metal ion solvation involves many subtleties of covalent versus electrostatic interactions [37-43]. Unfortunately, detailed insights into this rich and varied chemistry are often limited because theory and experiments cannot study the same systems in the same environment. Isolated metal complexes provide model systems, more tractable for theory, that can elucidate key interactions. Careful investigations of electronic structure, geometries, bonding energies, and reactivity are therefore possible. As discussed in this chapter, our research focuses on these model metal-molecular complexes and their clusters using molecular beam sources, mass spectrometers, and infrared laser spectroscopy, in combination with computational chemistry.

To investigate metal systems containing a specific composition, we study *ionized* clusters and complexes which can be mass selected. Isolated metal centers or those with specific numbers of attached ligand or solvent molecules can be produced and studied. Transition metal ion-molecule complexes have been studied with mass spectrometry for many years, providing reaction products and rates, as well as bond energies [44-57]. While these data are valuable, *spectroscopy* is needed on these systems, evaluated with corresponding computational studies, to make real progress in the understanding of metal electronic structure and bonding.

Vibrational spectroscopy provides the best probe of structure and bonding for metal complexes, and both IR and Raman have been employed for many years in this area [58,59]. However, while these methods are straightforward for conventional inorganic complexes [58], and can be adapted for adsorbates on surfaces [59], they are not easily applied to low density samples in the gas phase. Vibrational information can be obtained via electronic [60-81] or photoelectron spectroscopy [82-97], but IR spectra can be compared more directly to the predictions of theory. Small metal ions have been studied with infrared absorption spectroscopy in rare gas matrices [98], but the identification of the spectral carrier in these experiments can be ambiguous. Ionized complexes in the gas phase can be size-selected with mass spectrometers, but the resulting density is too low for absorption spectroscopy. Ion spectroscopy is often further complicated by the conditions in ion sources, generally involving discharges, hot plasmas, or other forms of energetic excitation. Until recently, these issues severely limited the IR spectroscopy of ions. However, much recent progress has been made in this area [99-118]. Improved ion sources employing laser ablation or electrospray ionization (ESI) now produce a wide variety of metal-ligand and metal-solvent complexes. Ion cooling, needed for sharp spectra, has been implemented with supersonic expansions or cryogenic ion traps. Sensitivity limitations have been addressed by using laser photodissociation spectroscopy rather than absorption. Finally, new IR lasers provide intense sources with broad tuning ranges to access the full vibrational spectrum [119,120]. Infrared spectroscopy of gas phase ions is now a rapidly expanding area of research, in which our group has been actively engaged.

Our experiments use laser vaporization in pulsed-nozzle/supersonic molecular beam sources to produce cold metal-containing ions [121]. Although other groups use electrospray ionization (ESI) sources, we find the laser source to be better suited to the ions we study. The ions produced are analyzed and mass selected with a specially designed reflectron time-of-flight spectrometer (RTOF) [122]. This instrument provides high throughput for maximized ion density, while maintaining the cold temperatures produced by the source. Selected ions are spatially bunched at the turning point in the reflectron field to optimize overlap with the laser. Excitation here allows the full mass spectrum to be detected for each laser shot so that different fragment channels can be recorded simultaneously. The experiment employs the high intensity, broadly tunable, optical parametric oscillator/amplifier (OPO/OPA) laser sold by LaserVision [119]. Its main configuration covers the range of 2000–4500 cm^{-1}, corresponding to the higher frequency vibrations of small ligand or solvent molecules. A second OPA configuration employs silver-gallium-selenide crystals,

extending the tuning range to the 600–2300 cm^{-1} region [120]. Here, we study lower frequency ligand or solvent vibrations, as well as the M–O stretches of oxide clusters. The two laser configurations allow almost full coverage of the infrared spectrum. Combined with our ion source and mass spectrometer, these lasers have produced spectroscopy for many transition metal-molecular complexes [106,107,123-169]. This work is complemented by that of other groups using similar infrared OPO laser systems [108-118,170-200] or free-electron lasers (FELs) [201-212].

This kind of mass spectrometry combined with IR spectroscopy provides the coordination numbers, geometries and electronic structures of metal-molecular complexes. Mass spectra and photodissociation patterns reveal the number of ligand or solvent molecules attached to a specific metal center. The vibrations in these complexes typically occur near those of the corresponding free ligand or solvent molecules, indicating that binding usually takes place without dissociation or insertion chemistry. The number of IR bands, their shifts compared to the vibrations of the isolated ligand or solvent molecules, and the relative band intensities provide distinctive patterns that can be compared to the predictions of theory to determine structures. Density functional theory (DFT) is employed for these studies, although we use due caution in its applications. For example, a well-known issue for transition metal complexes is determination of the correct spin configuration giving rise to the ground state [213-219]. DFT has trouble with the relative energies of spin states, but usually predicts a valid infrared pattern for each spin state. The measured vibrational patterns are then compared to the (scaled harmonic) predictions of theory for different electronic states. These vibrational patterns, rather than the computed relative energies, are then generally good enough to determine the spin of the ground state or to reveal the presence of more than one electronic state. Infrared patterns can also reveal the occurrence of intracluster reactions through the appearance of new spectra corresponding to reaction products.

A key aspect of this work is the ligand or solvent molecule binding energy and our ability to cause fragmentation with IR photons. Dissociation energies for many metal ion complexes are known via methods such as collision induced dissociation [44-55]. Bond energies range from 5000 cm^{-1} (12–15 kcal/mol) for electrostatically bonded metal-CO_2 ions up to as high as 30,000 cm^{-1} (70–80 kcal/mol) for metal-benzene complexes with strong covalent bonds. Across this range, one-photon infrared excitation on vibrational fundamentals is not energetic enough to cause photodissociation. Bond energies usually decrease in complexes with more ligands, but these systems have the same problem until the metal coordination is completed. However, when

ligands are present beyond the coordination, they are bound by weaker electrostatic forces and their elimination is efficient, providing good spectra. The onset of greater dissociation yields therefore identifies the coordination number. To study smaller complexes with partial coordination and stronger bonding, we attach weakly-bound rare gas atoms, using the "tagging" method first employed by Lee and coworkers [99-101]. This general method is now used throughout ion spectroscopy [102-118]. To document the effects of tagging, we use theory to investigate the spectra of complexes with and without the tag atom.

Another essential requirement for this work has been the extension of IR laser coverage to the fingerprint region. In the past, this could only be done using FEL's, such as the FELIX system in the Netherlands. Previous studies there by our group and others used infrared resonance enhanced *multiphoton* dissociation (IR-REMPD) of cations to obtain vibrational spectra [201-212]. However, the quality of these spectra is often poor because of the laser line width and power broadening from the multiphoton processes. The new OPO's have broader wavelength coverage (600–4500 cm^{-1}) and higher resolution. Using tagging, or elimination of external ligands, spectra can be measured via *single photon* dissociation, and line widths are much improved (1–5 cm^{-1}, limited by predissociation). As shown in Figure x.1, the quality of the spectra obtained now is excellent.

In this chapter, we describe the work from our lab investigating metal ion complexes with carbon monoxide [143-155], carbon dioxide [123-128], water [129-142], acetylene 156-162], and benzene [165-168]. These experiments show that IR photodissociation spectroscopy can be applied to ions containing virtually any metal or ligand. It provides the dissociation products, the number of IR-active vibrations, the frequency shifts that occur when ligands bind to metal, and the relative intensities of different bands. Computational chemistry complements the experiments, predicting the structures of complexes, their electronic configurations, and their spectra.

x.2 Metal-Carbonyl Complexes

Transition metal carbonyls provide classic examples of inorganic complexes [7-11], and CO is the classic probe molecule for surface science and catalysis [1-3,58]. In both contexts, the carbonyl stretch reveals the nature of the bonding. Metal carbonyls are characterized by the positions of the C–O stretch relative to the vibration of the isolated CO diatomic (2143 cm^{-1})

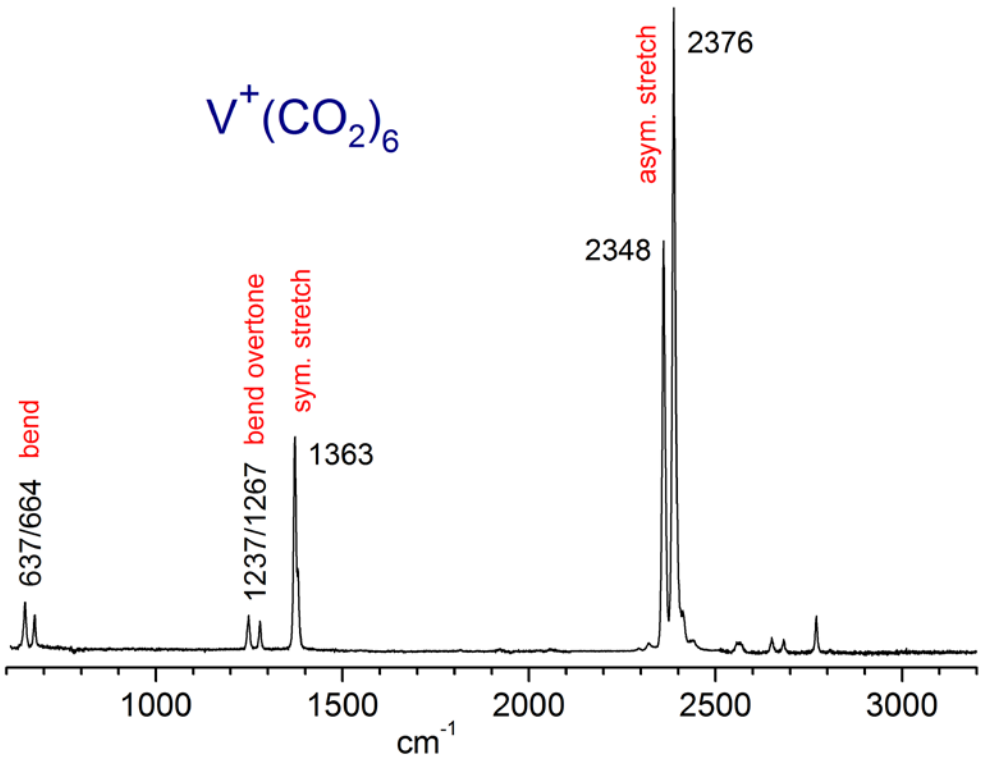

Figure x.1. The infrared spectra of $V^+(CO_2)_6$ complexes, illustrating the broad tunability of our IR-OPO lasers. The CO_2 bend and asymmetric stretch have two bands corresponding respectively to molecules coordinated to the metal ion and those attached only to other CO_2 molecules. The symmetric stretch is only IR active for molecules attached to the metal and a single band is observed here.

[220]. Unsaturated carbonyls, including ions, have been investigated by mass spectrometry [45-55,221-226], matrix isolation spectroscopy [98], and photoelectron spectroscopy [82,83,85,87]. Computational studies have explored the mechanism of the shifts that occur for the C–O stretches in different systems, including the familiar effects of σ donation and π back-bonding [219,227-235]. Our group has investigated transition metal carbonyl *cations* [143-155] to compare these to well-known neutrals. Other research groups have employed similar methods to investigate other atomic metal cation-carbonyls [190-197] or the carbonyls of metal atom clusters [205-209].

We first studied cation complexes that could provide isoelectronic analogs to known neutral metal carbonyl complexes. $Co^+(CO)_5$ complex provided an analog to $Fe(CO)_5$ [145], $Mn^+(CO)_6$ provided an analog to $Cr(CO)_6$ [147], and $Cu^+(CO)_4$ provided an analog to $Ni(CO)_4$ [150]. In each case, the cations were found to have the same coordination and structures as the

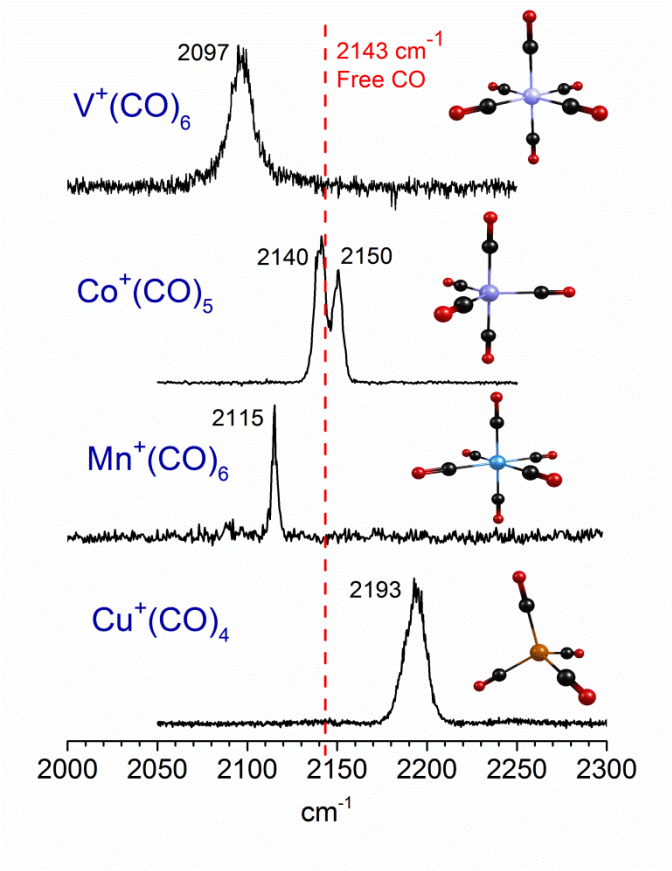

Figure x.2. The infrared spectra of the saturated carbonyl complexes for selected metal cations. The red dashed line shows the frequency of the isolated CO molecule.

corresponding neutrals (trigonal pyramid, octahedral, and tetrahedral, respectively) and the same closed-shell singlet ground states. However, significant differences were apparent in the spectroscopy between the neutrals and the corresponding cations. In the neutrals, the C–O stretch vibrations are strongly red-shifted compared to the stretch of molecular CO by 100–150 cm^{-1}. However, as shown in Figure x.2, the C–O stretch vibrations were hardly shifted at all for the Co and Mn cations and they were *blue*-shifted for the Cu cations. The frequencies for these neutrals and ions are summarized in Table x.1. It is well known in inorganic chemistry that the shifts of the C–O stretches arise from the competing effects of σ donation and π back-bonding [219,227-235]. For most neutral metals, π back-bonding is the more significant factor, and the carbonyl stretches occur at much lower frequencies than that of CO itself. The smaller red shifts seen for the cations here are attributed to their reduced π back-bonding [149]. Blue shifts to higher frequencies are known to occur for certain metals with filled *d* shells that are inefficient at

Table x.1. A comparison of the carbonyl stretch frequencies for isoelectronic neutral and cationic complexes.

Complex	Experimental C–O stretch (cm^{-1})
$Cr(CO)_6$	2003 [236]
$Mn^+(CO)_6$	2115
$Fe(CO)_5$	2013, 2034 [237]
$Co^+(CO)_5$	2140, 2150
$Ni(CO)_4$	2056 [238]
$Cu^+(CO)_4$	2193

back donation. We find this behavior for the copper carbonyl cations shown here [150], but also for Au^+, Pt^+ and Rh^+ carbonyl complexes [143,144,155].

The fully coordinated ions and their corresponding neutrals shown in Table x.1 all have the 18-electron configuration, which is recognized as a guiding principle in transition metal chemistry. We were also interested to see how robust this rule is, and what its limitations are, if any. Early transition metals have fewer valence *d* electrons, and therefore would require more carbonyl ligands to achieve the 18-electron configuration. We investigated the cation carbonyls of the group V metals (V, Nb, Ta) [146,151], which would need seven carbonyls to reach this limit, and those of Sc and Y [154], which would need eight carbonyls, to see if such higher coordination numbers were possible. According to theory, these higher coordination complexes are stable for each of these metals. However, we found experimentally that vanadium did not form the seven-coordinate (7C) carbonyl, but instead formed the six-coordinate (6C) complex (see spectrum in Figure x.2). Niobium and tantalum, on the other hand, did form the 7C complexes. The spectrum of $Ta^+(CO)_7$, which forms a capped octahedral structure rather than the pentagonal bipyramid, is presented in Figure x.3. Likewise, scandium did not form the 8C complex, but yttrium did. In both groups, only the heavier metals formed the expected high coordination. We explained this trend in terms of the kinetics of carbonyl addition to these metals. In both systems, the filled coordination produces a singlet ground state, while the n−1 complex is a triplet. Adding the last CO therefore requires a spin change, which may inhibit the

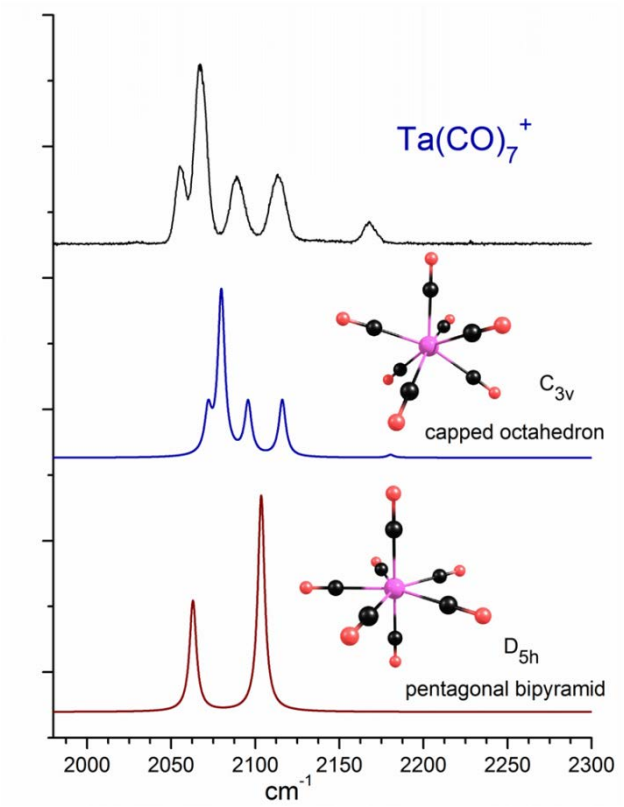

Figure x.3. The infrared spectrum of $Ta^+(CO)_7$ compared to the spectra predicted by density functional theory for two different isomers. The spectrum agrees with that predicted for the capped octahedron structure.

rate of this process. Our clusters grow in a 1–3 microsecond time frame (defined by the pulsed jet expansion) by sequential addition of ligands to the ablated metal cations, and therefore slower growth rates may inhibit the formation of complexes, even if they are stable. The heavier metals with stronger spin-orbit coupling should change spin more readily, possibly explaining how these species could achieve the higher coordination. This reasoning was employed previously by Weitz and coworkers to explain similar results for CO addition to unsaturated neutral carbonyls [239,240]. Harvey and coworkers used computational studies to model these spin-controlled kinetics [241-243]. Since our work on these systems, Zhou and coworkers have found eight-coordinate complexes for other early transition metal cations [196], and they have found unexpected 8C complexes for the alkaline earth metal cations [197].

The group IV metals (Ti, Zr, Hf) all have an odd number of electrons as cations, and it is therefore unclear what coordination would be expected for these systems. We found that they all formed 6C complexes rather than the 7C (17-electron) or 8C (19-electron) species [152,195]. Rhodium carbonyls provided another interesting case [155]. Rh^+ is a d^8 species, which is generally expected to form 4C square planar complexes [11], even though the 18-

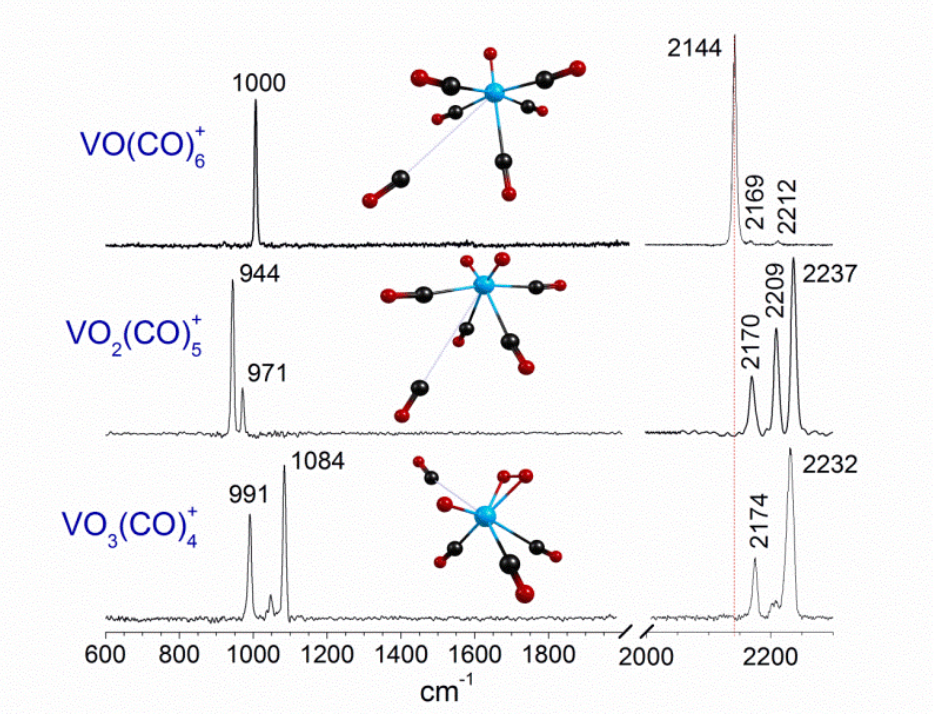

Figure x.4. The IR spectra of vanadium oxide carbonyls and the structures predicted to be most stable for these complexes. Each complex has one external ligand, which is eliminated in the photodissociation process to obtain the spectrum. The C–O stretch vibrations are shifted to the same or higher frequencies than the free-CO vibration, indicated as the dashed red line. The bands at 2169–2174 cm^{-1} come from the external CO ligand.

electron species would be 5C. We found a primary coordination of four carbonyls but a secondary coordination of five. The fifth ligand had an intermediate binding energy, weaker than the first four, but not as weak as the external ligands. The spectrum of the n = 4 complex indicated a square-planar structure, while that of the n = 5 species was a square pyramid.

We have also studied metal oxide carbonyls. Oxidation of the metal center removes the *d* electron density available for back-bonding, which reduces or eliminates the red shifts in these systems. The $V^+(CO)_6$ complex spectrum has a slightly red-shifted C–O stretch, with one main band because of the octahedral structure [146,151]. $VO^+(CO)_5$, $VO_2(CO)_4^+$ and $VO_3(CO)_3^+$ (each measured by elimination of one excess CO from the next-larger complex) have C–O stretches shifted progressively further to the blue because of the reduced back-bonding (Figure x.4) [153]. Similar blue-shifted carbonyl stretches are observed for CO binding on metal oxide surfaces [2,59]. The metal-oxygen stretches in these clusters can be compared to those of the corresponding VO^+, VO_2^+ and VO_3^+ ions recently measured by Asmis and coworkers [244]. The oxide stretches in the carbonyls shift to the red compared to those in the isolated oxides, another result of partial charge transfer in these systems.

x.3 Metal-CO_2 Complexes

The binding of CO_2 to metals is of widespread importance for CO_2 capture and conversion to small organics [20,21,25,25,34,35]. However, the binding of CO_2 to metal ions in the gas phase involves primarily electrostatic interactions [245-247], and these systems have been studied less than the corresponding carbonyl complexes. Our lab has studied the electronic spectroscopy of $Mg^+(CO_2)$ [65] and $Ca^+(CO_2)$ [67], and the infrared photodissociation spectroscopy of several $M^+(CO_2)_n$ cation complexes [123-127]. Figure x.1 shows the infrared spectrum of $V^+(CO_2)_6$ which illustrates the behavior seen for many of these systems. Of the normal modes for CO_2, the degenerate bending mode (ν_2, 667 cm^{-1}) and the asymmetric stretch (ν_3, 2349 cm^{-1}) are IR active for the isolated molecule, whereas the symmetric stretch (ν_1, 1333 cm^{-1}) is inactive [248]. However, theory and experiments agree that metal cation binding is most favorable in the M^+-O=C=O linear configuration. In this structure, all three vibrations are IR active. As shown in the figure, CO_2 molecules attached to metal have these three vibrations, with shifts to higher frequencies than the vibrations of the isolated molecule. In a cluster like $V^+(CO_2)_6$, there are coordinated molecules, which give rise to shifted vibrations, and second-sphere molecules not attached to the metal whose vibrations are mostly unshifted. This gives rise to doublet features (shifted plus unshifted bands) for the asymmetric stretch and bending vibrations, and a single band (shifted only) for the symmetric stretch, which is only IR-active when it is attached to the metal. This pattern of bands has been seen for almost all the metal ion-CO_2 complexes that we have studied.

An exception to this general behavior occurs in larger $V^+(CO_2)_n$ clusters, in which additional bands were seen beyond the coordination and solvation features. As shown in Figure x.5, new bands at 1140, 1800, 2402, and 3008 cm^{-1} were seen for clusters with seven or more CO_2 ligands, and these bands became more intense in the larger clusters. These new bands suggest that there was an *intracluster reaction* producing a new kind of structure. Because the clusters were mass-selected, the reaction product must have the same mass as one or more CO_2 units, which could be true for an oxide-carbonyl species, $VO^+(CO)(CO_2)_{n-1}$, a metal carbonyl-carboxylate species, $V^+(CO)(CO_2)_{n-1}(CO_3)$, or a metal oxylate species, $V^+(CO_2)_{n-2}(C_2O_4)$. To explore these possibilities, we made the oxide-carbonyl species directly, and found that the VO^+ and carbonyl stretches in these systems (Figure x.4) do not match the new bands. Instead, we

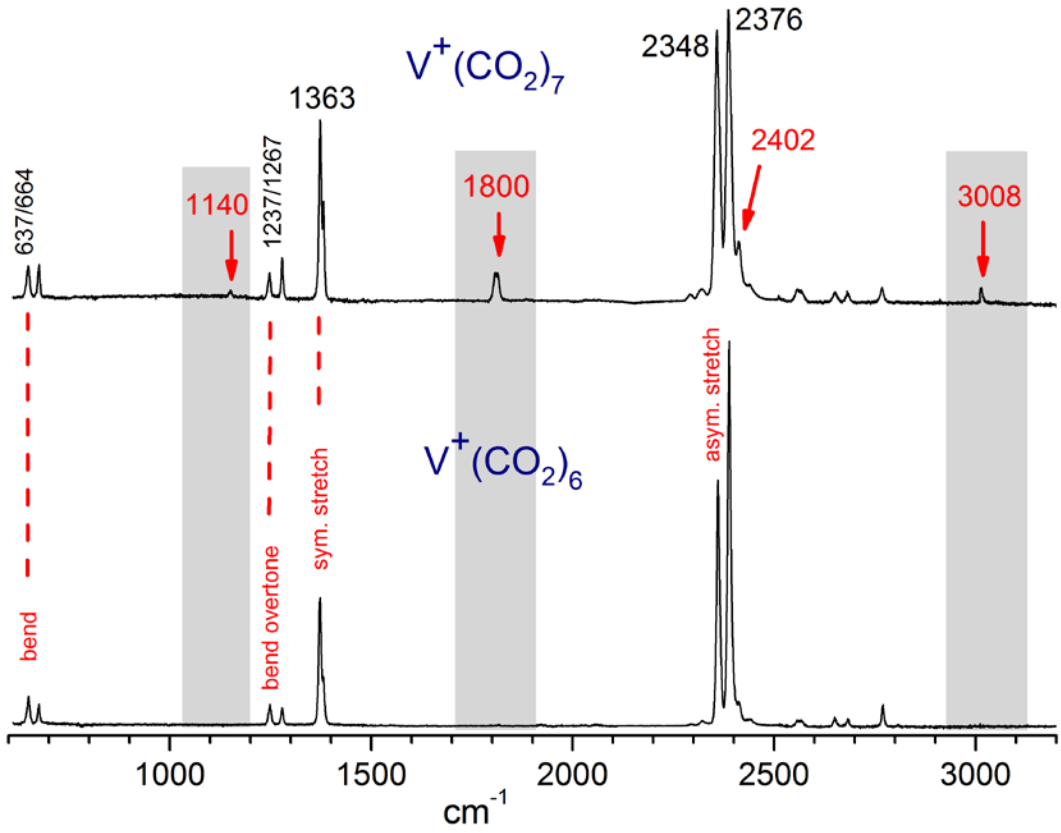

Figure x.5. The infrared spectrum of $V^+(CO_2)_7$ compared to that for $V^+(CO_2)_6$ showing the sudden appearance of several new vibrations associated with an intracluster reaction.

found that the reaction product is an oxalate species ($C_2O_4^-$), with covalently linked CO_2 molecules. The lower frequency vibrations (1140 and 1800 cm^{-1}) are those of the oxalate moiety, and the higher frequency vibrations (2402 and 3008 cm^{-1}) are those of solvating CO_2 molecules interacting with the new kind of charge center in the clusters. Although we cannot determine the exact charge states in this system, oxalate is most stable when it carries a negative charge. This reaction therefore apparently occurs by electron transfer from the V^+ ion to CO_2, producing a V^{2+},$C_2O_4^-$ ion pair. This suggestion would explain the onset at larger cluster sizes. Solvation from the surrounding excess CO_2 molecules could stabilize the higher charge state of V^{2+} and that of the oxalate. Theory on this system is plagued by multi-reference issues, and we were not able to determine whether the ion pair is in contact or solvent-separated. However, this same kind of chemistry has also been seen by Weber and coworkers [174] for negative ion $M^-(CO_2)_n$ clusters. Apparently, the negative charge on CO_2 activates it to enable a rich variety of chemistry.

x.4. Metal-Water Complexes

The interaction of water with metal ions is fundamental to the chemistry of solvation [12-14,37-43]. Unfortunately, the details of cation-water interactions are difficult to obtain from solution measurements, which involve ensemble averaging over many structures. Gas phase measurements have investigated the thermochemistry of cation-water bonding [47,48,50,54,55,249-264], and computational studies have studied structures and energetics of these systems [57,265-277]. However, infrared spectroscopy probes the structures of these systems more directly. Our work has examined several $M^+(H_2O)_n$ and $M^{2+}(H_2O)_n$ systems [129-142], focusing on both the mono-hydrated complexes and the coordination behavior when multiple water molecules condense around the metal ion. Other groups have explored these same kinds of systems using similar methods [170-173,178-181,183-187,192].

We have studied nearly all of the singly-charged first-row transition metals in complexes with a single water molecule [129-142]. The spectra in the O–H stretching region are shown in Figure x.6. The binding energies of argon are very different for the early vs late transition metals. Consequently, the late transition metals require the attachment of two or more argon atoms before photodissociation can be measured in this region of the IR. As shown in the left frame of the figure, those complexes tagged with a single argon have more complex vibrational patterns than those tagged with two argons. The additional structure at higher frequency arises from partially-resolved rotational structure (K-type bands) on the asymmetric stretch band. This structure is discussed in more detail below. We found that water bound to metal ions generally has O–H stretching frequencies that are shifted to the red compared to those of the free molecule (3657, 3756 cm^{-1} for the symmetric and asymmetric stretches) [248]. In a charge-transfer process not unlike that for metal carbonyls, the cation polarizes water, removing electron density from its highest occupied molecular orbital. This orbital involves the non-bonding lone pairs on oxygen, but also has bonding character along the O–H bonds; weakening these bonds lowers the vibrational frequency. Figure x.7 shows an electron density map for the $Ti^+(H_2O)$ complex in its doublet ground state compared to that in the separated cation/molecule system. This illustrates the effects of the charge transfer between the water and the metal. As shown in the two views, electron density increases on the metal ion center, and decreases in the vicinity of the O–H bonds. This charge transfer drives the shift in the vibrational frequencies. In addition to the

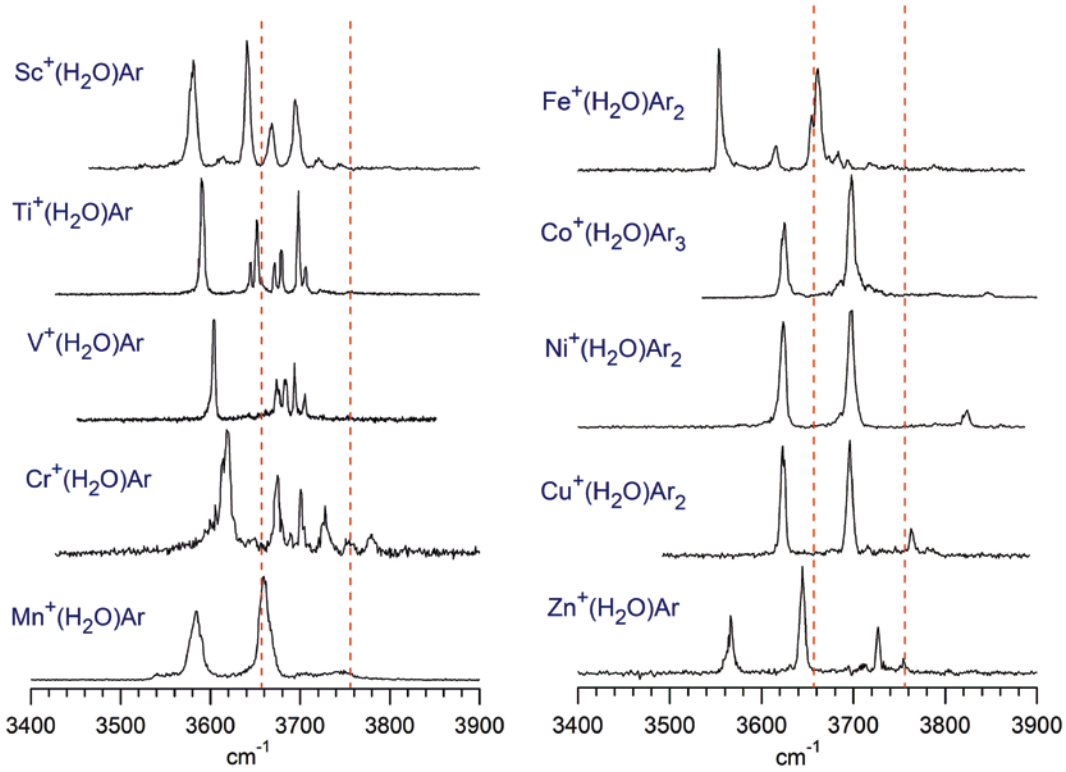

Figure x.6. The infrared spectra in the O–H stretching region for different transition metal cation-water complexes compared to the symmetric and asymmetric O–H stretch frequencies for the isolated water molecule (dashed red lines). The early transition metal complexes are tagged with a single argon, producing partially resolved rotational structure in some cases, whereas the late-transition metal complexes are usually tagged with two or three argons. The spectra for the early transition metal complexes are generally shifted further to the red than those of the late transition metals. The lowest frequency band for $Fe^+(H_2O)$ is from an isomer with argon attached to an OH of water, inducing an even greater red shift [130].

redshift in the frequencies, which varies considerably with different metals, the relative intensities of the two O–H stretches change, with the symmetric stretch gaining relative to the asymmetric. In the free water molecule, the asymmetric:symmetric stretch intensity ratio is about 18:1, whereas in the cation water complexes this ratio is closer to 1:1. The symmetric stretch in these metal complexes oscillates charge more effectively along the molecular axis, enhancing the dynamic dipole and the IR intensity. The shifts seen for these singly charged metal complexes have been compared to selected examples of doubly charged complexes [135,137-139]. In those systems, the shifts of the vibrational frequencies and the enhancement of the symmetric stretch intensity are both greater than they are for the corresponding singly charged complexes.

Interestingly, the shifts of the O–H stretching frequencies measured are generally greater for the early transition metals than they are for the late transition metals. Figure x.8 shows a plot of the

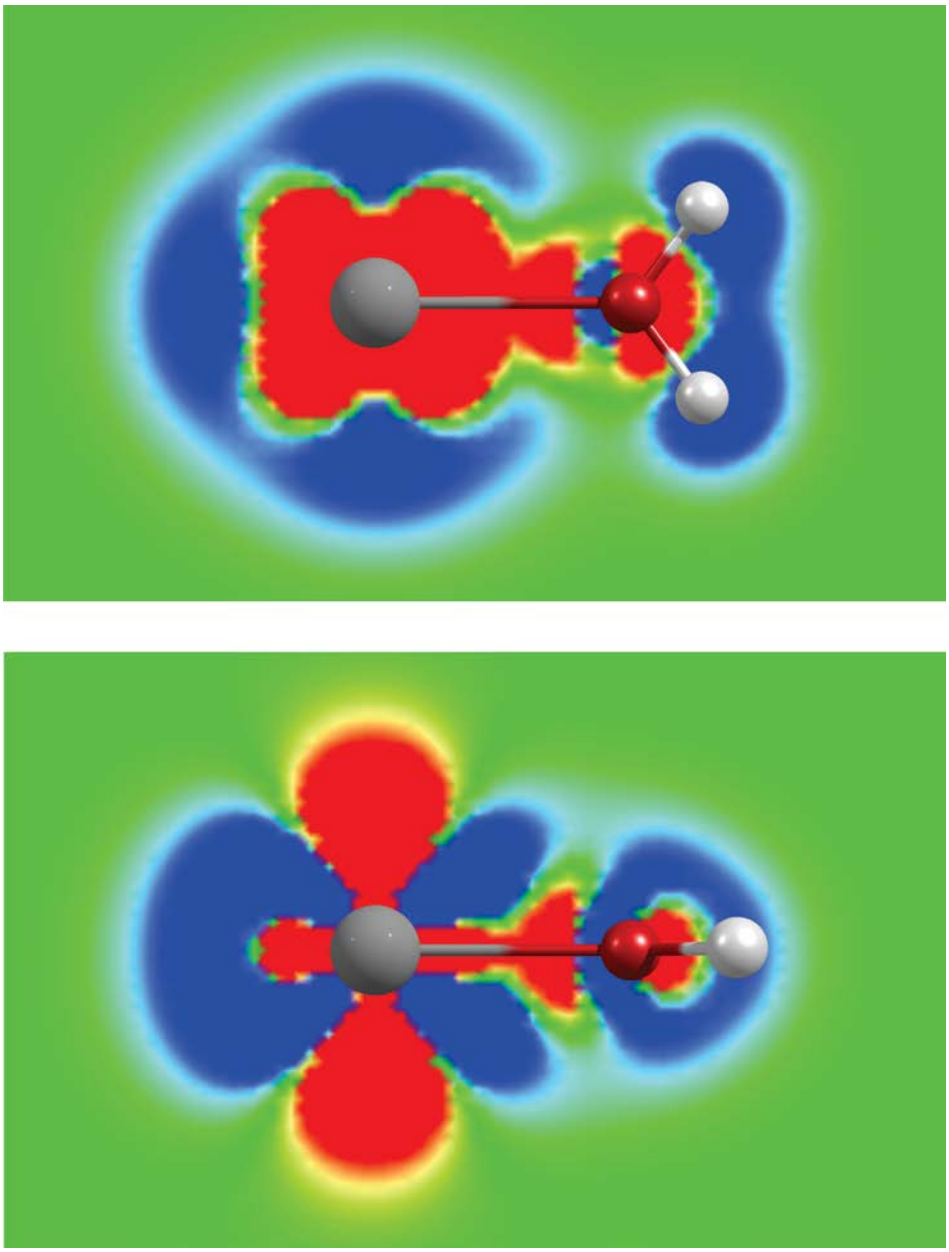

Figure x.7. The charge density map for the $Ti^{+}(H_2O)$ complex in its doublet ground state. Red coloring shows an increase in charge density compared to the separated cation-water system, whereas blue shows a reduction in charge density.

O–H stretch frequencies across the periodic table groups and a comparison to the corresponding M^{+}-(H_2O) bond energies determined in other labs. Surprisingly, the magnitudes of the red-shifts for the two O–H stretches of water are greater for the early transition metal, and less for the late transition metals, with a local maximum for the manganese cation. The binding energies are greater for the late transition metals. It therefore seems that there is no clear correlation between binding energies and vibrational band shifts, even though the charge transfer that causes the vibrational

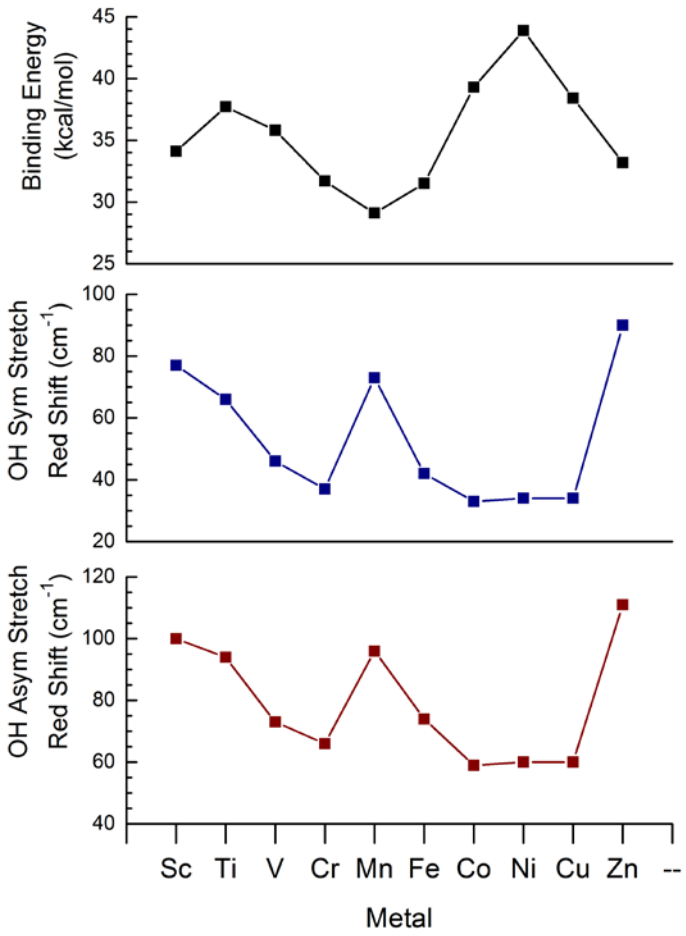

Figure x.8. Plots of the shifts in the O–H stretches for different transition metal cation-water complexes compared to the cation-water binding energies.

shifts should have at least some relevance for the electrostatic bonding in these systems. However, the bonding in these transition metal-water complexes is a complex mixture of both electrostatic and covalent interactions, and so it may be oversimplified to assume a correlation between these two properties. It is worth noting that density functional theory accurately predicts both the trends in binding energies and vibrational frequency shifts.

In Ar-$M^+(H_2O)$ complexes when the tag atom binds opposite water, the complex has C_{2v} symmetry and is nearly a symmetric top, with only the light hydrogen atoms located off the C_2 symmetry axis. This causes the *A* rotational constant to be relatively large (>10 cm^{-1}) and K-type rotational sub-band structure can be resolved, even with our modest 1 cm^{-1} laser linewidth. This is apparent in the spectra for the early transition metals, in the left frame of Figure x.6, with the exception of the $Mn^+(H_2O)$ spectrum (it binds argon in a bent position, which produces a much smaller *A* constant, and the structure is not resolved [138]). In these systems, a multiplet

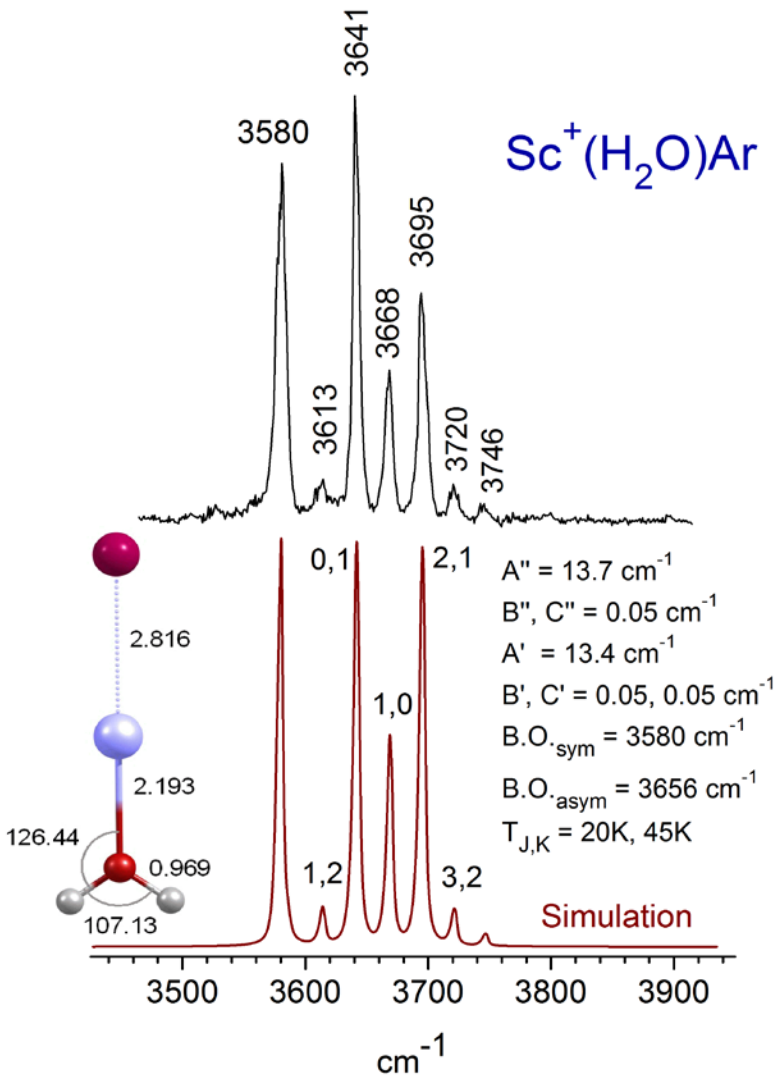

Figure x.9. An expanded view of the IR spectrum in the O–H stretching region for scandium-water cations compared to a simulated spectrum including partially resolved rotational structure. The rotational structure is consistent with expectations for a C_{2v} structure, with a triplet for the asymmetric stretch and a 3:1 intensity alternation from the nuclear spin statistics. A, B, and C are the rotational constants in the ground (") and excited (') vibrational states, and B.O. indicates the band origins. B and C values come from the theoretical structure, whereas the A values are adjusted to fit the spacings in the spectrum. The temperature is adjusted to fit the relative band intensities (T_K) and line widths from unresolved structure (T_J) in the spectrum. Figure used from reference 137 with permission of the American Institute of Physics, Copyright 2011.

structure arises for the asymmetric stretch, which is a perpendicular-type band. The symmetric stretch is a parallel-type band, with more closely spaced rotational structure that cannot be resolved under these conditions. Because the hydrogens of water are equivalent by symmetry, ortho-para symmetry rules must be applied, resulting in a 3:1 statistical weight for transitions originating in the K = 1 vs K = 0 levels. At low temperature, only the K = 0 and 1 levels are

populated significantly, and K = 1 cannot relax to K = 0 because of the nuclear spin symmetry. The only transitions seen are those originating from these two levels. The K" = 0 → K' = 1 transition (labelled 0,1 in the figure) is then lower in relative intensity than the K" = 1 → K' = 0 or K" = 1 → K' = 2 transitions (labelled 0,1 and 2,1 in the figure). The rotational structure can be simulated using the PGopher software [278], and parameters adjusted to get the best match with the experiment, as shown in Figure x.9. The best fit produces the *A* rotational constant and the temperature of the ions. As shown in the figure, the non-equilibrium conditions of the supersonic molecular beam produces slightly different temperatures for the J and K quantum states, an effect that is not uncommon in such molecular beam experiments. Assuming that the O–H bond distances remain nearly constant (suggested by theory), then the *A* rotational constant reveals the H-O-H angle, which is often expanded by the cation-water polarization interaction. In the scandium example shown here, this angle is estimated to be 107.13°, which is significantly larger than the angle in an isolated water molecule (104.7°). Our rotationally resolved studies on the Sc^+, Ti^+, V^+, Nb^+, and Cr^+ systems all found H-O-H angles expanded with respect to that of water [135,137,141,142]. In the case of the vanadium and niobium complexes, the analysis of the rotational structure was complicated by an unexpected quenching of the ortho-para separation catalyzed by the metal ions, changing the selection rules and the appearance of the spectra [142].

IR spectroscopy of metal cations solvated by multiple water molecules can reveal their coordination numbers. In small clusters, water coordinated directly to metal has free O−H stretching vibrations near those of the isolated water molecule. However, when water adds to the second sphere, hydrogen bonding causes a strong red shift of 200–400 cm^{-1} in the O–H stretches, and the IR intensity increases. The first appearance of vibrations in the hydrogen bonding region therefore identifies the coordination number for the metal cation. We found in the past that this is four water molecules for Ni^+ [132], and three for Zn^+ [140]. Figure x.10 shows spectra for different sizes of $V^+(H_2O)_n$, in which the first evidence for a band in the hydrogen bonding region occurs for the n = 4 cluster, indicating that the coordination is complete with three molecules [278]. In related work, Nishi and co-workers studied $V^+(H_2O)_n$ complexes without tagging, finding a coordination of four molecules [172]. Our result here can be rationalized to agree with their result, if we assume that argon acts as a coordinating ligand in at least some of the n = 4 complexes. V^+ ions exhibited a coordination of six for carbonyl ligands [146,151] and

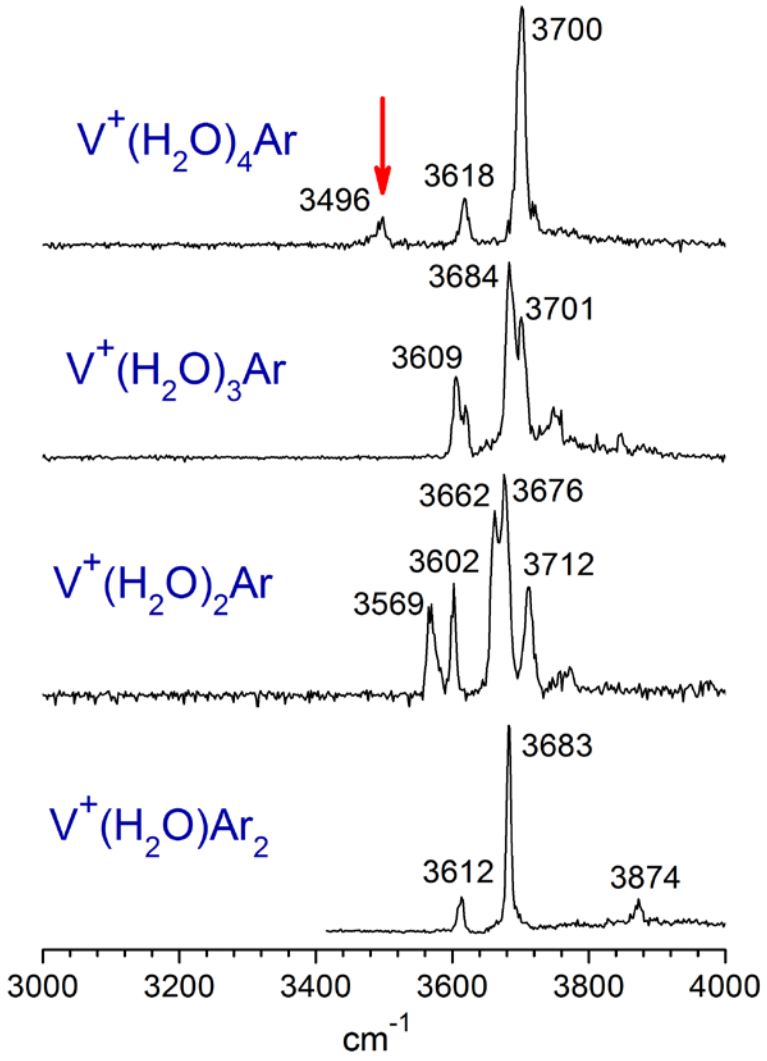

Figure x.10. Infrared spectra for $V^+(H_2O)_n$ clusters in the n = 1–4 size range. The first evidence for a band in the hydrogen bonding region occurs for the n = 4 cluster, with the band at 3496 cm^{-1} marked with the red arrow. This suggests that the solvation sphere is filled with the next-smallest n = 3 cluster.

four for CO_2 ligands [127], contrasting with the behavior seen here for water. Coordination numbers for the singly positive ions we have studied are generally lower than those expected for the more highly charged metal ions found in normal solutions. The highly charged metal ions in solution have fewer electrons occupying the valence orbitals than the singly charged species. It is likely that ligand-electron repulsion from the occupied orbits causes the lower coordination numbers for the singly charged species.

x.5. Metal-Acetylene Complexes

Metal-acetylene and metal-ethylene complexes form the simplest examples of cation-π interactions relevant in many areas of catalysis and biological chemistry [6-11,16,280-283]. These systems have been studied often in ion chemistry and investigated with computational chemistry [284-289]. In some of the first spectroscopic work, our group measured electronic spectra for $Ca^+(C_2H_2)$ and $Mg^+(C_2H_2)$ complexes [69,70]. In the infrared, we investigated the C−H stretches in several transition metal ion complexes with a single acetylene [157], comparing the vibrations to the known symmetric and asymmetric stretches of acetylene (3374 and 3289 cm^{-1}, respectively) [248]. Figure x.11 shows a comparison of several $M^+(C_2H_2)$ complexes, including new examples from more recent work. As shown in the figure, all the C–H stretches for these metal ion complexes occur at frequencies lower than those of acetylene itself. The cation-π interaction transfers charge from the molecule to the metal in much the same way seen already for metal-carbonyls and metal-water complexes. In acetylene complexes, polarization removes electron density from the C–C and C–H bonds, lowering their frequencies. The C–C and symmetric C–H stretches of acetylene are not IR active in the free molecule, whereas the asymmetric C–H stretch is IR-active. However, in cation-acetylene complexes, the C–C and symmetric C–H stretches can become weakly IR active from the distortion of the molecule (e.g., CH groups bending away from linear) or the changing dipole produced by concerted metal and molecular motion. Consequently, the spectra shown in Figure x.11 have stronger asymmetric stretch vibrations at lower frequency and weaker symmetric stretch bands at higher frequency. The intensity of the weaker symmetric stretch band varies for different metals depending on the degree of "activation" induced by the metal. The exception to this trend is the $V^+(C_2H_2)$ complex, which has two bands with nearly equal intensities. This suggests that the bonding in this complex is somehow different from that in the other species here.

Computational studies were insightful for these systems. We found that most metals form cation-π complexes, with the cation in a two-fold position above the π cloud and some slight bending of the CH groups away from the metal. However, the V^+ complex formed a very different structure – that of a VC_2 *metallacycle* with the CH groups bent strongly away from the metal (computed CCH angle = 37.7°). In this bent configuration, both C−H stretches are IR active with comparable intensity and there are much greater red shifts in the two frequencies, all

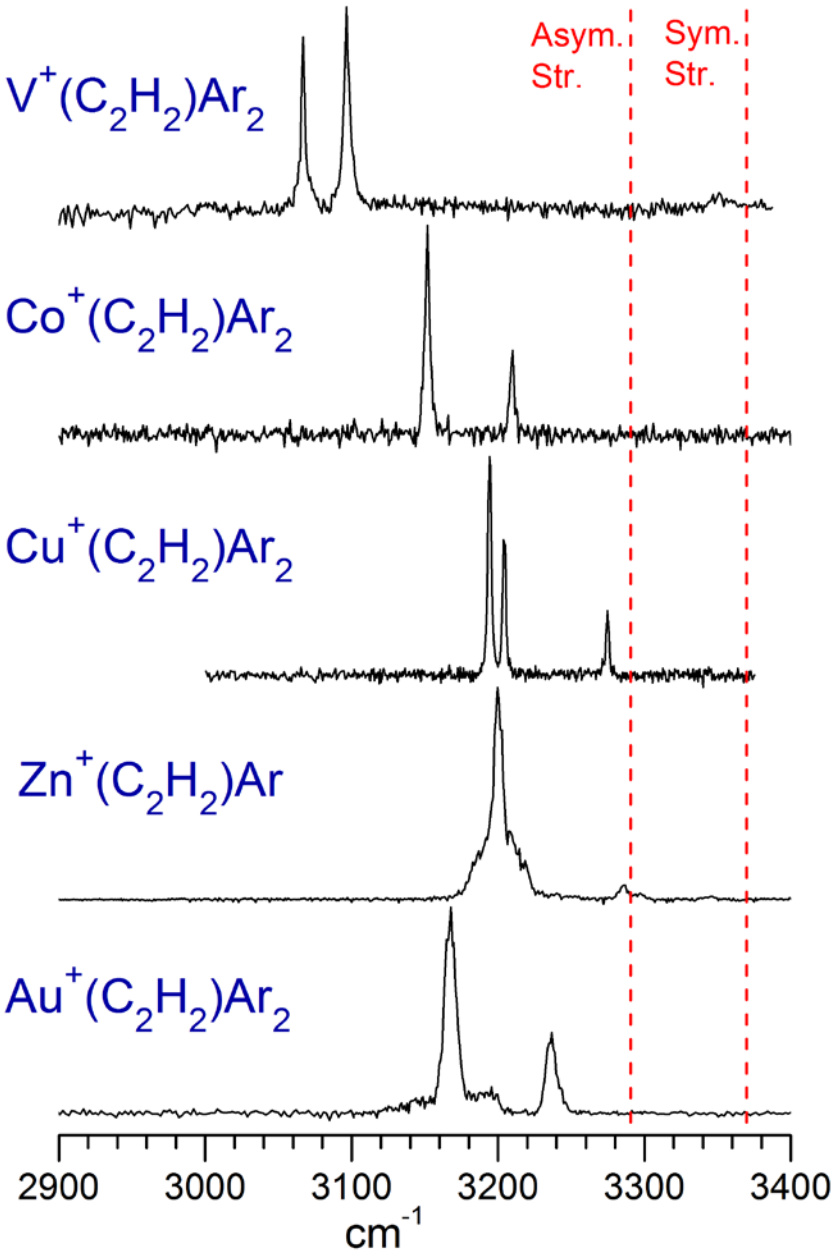

Figure x.11. Infrared spectra of cation-acetylene complexes in the C–H stretching region.

consistent with the experimental spectrum. There are covalent bonds between the metal and the carbons, and the C–C bond has lengthened (computed from 1.199 in acetylene to 1.301 Å in V^+-acetylene), consistent with its reduced bond order. The interaction between V^+ and acetylene is clearly very different from that of the other metal ions studied so far.

Complexes with multiple acetylene molecules coordinated to a single metal ion make it possible to investigate the coordination sphere and possible reactions between ligands mediated

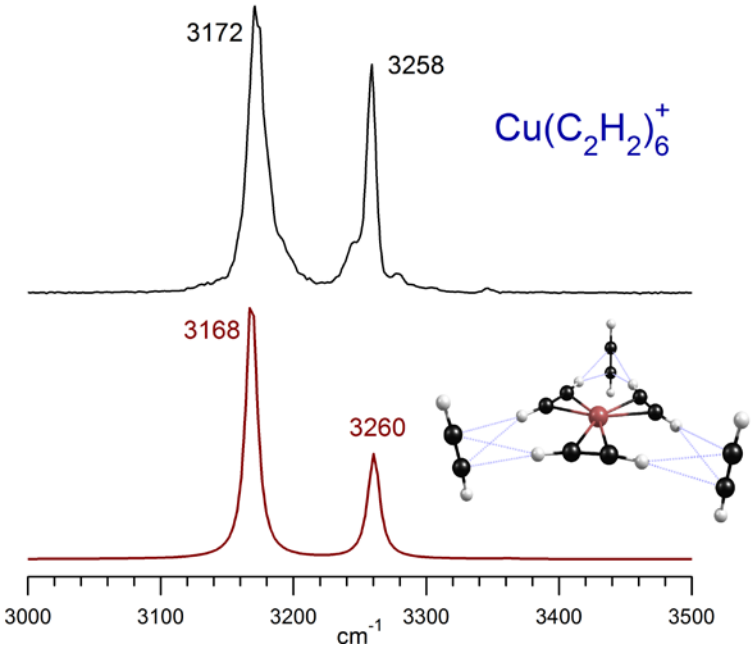

Figure x.12. The infrared spectrum of $Cu^+(C_2H_2)_6$ and the spectrum predicted by theory for the structure with three inner-sphere and three outer-sphere molecules. Figure used from reference 159 with permission from the American Chemical Society, Copyright 2015.

by the metal. In the case of multi-acetylene complexes of Ni^+, a coordination of four acetylenes was determined in a near-tetrahedral structure [158]. In larger clusters, a new band appeared which indicated an intracluster reaction forming cyclobutadiene [156]. In recent work, we examined the multi-acetylene complexes of Cu^+, finding an inner coordination of three acetylenes and a secondary solvation of three additional acetylenes in the highly symmetric $Cu^+(C_2H_2)_6$ complex [159]. In this structure, whose spectrum is shown in Figure x.12, each acetylene molecule in the second coordination sphere is bonded to two inner-sphere molecules via bifurcated CH-π hydrogen bonds. Because of the highly symmetric structure, the IR spectrum has only two bands corresponding to the in-phase and out-of-phase asymmetric stretches of the core (3172 cm^{-1}) and outer (3258 cm^{-1}) ligands. Gold cation also forms a three-fold inner sphere coordination, but with less symmetric second-sphere structures [160].

As noted above, the interaction between vanadium ions and acetylene molecules is quite different from that of the other transition metals, prompting us to examine its behavior as multiple acetylenes are added around the metal. Figure x.13 shows some of the spectra and structures obtained. The di-acetylene complex forms a bow-tie structure with each of the two

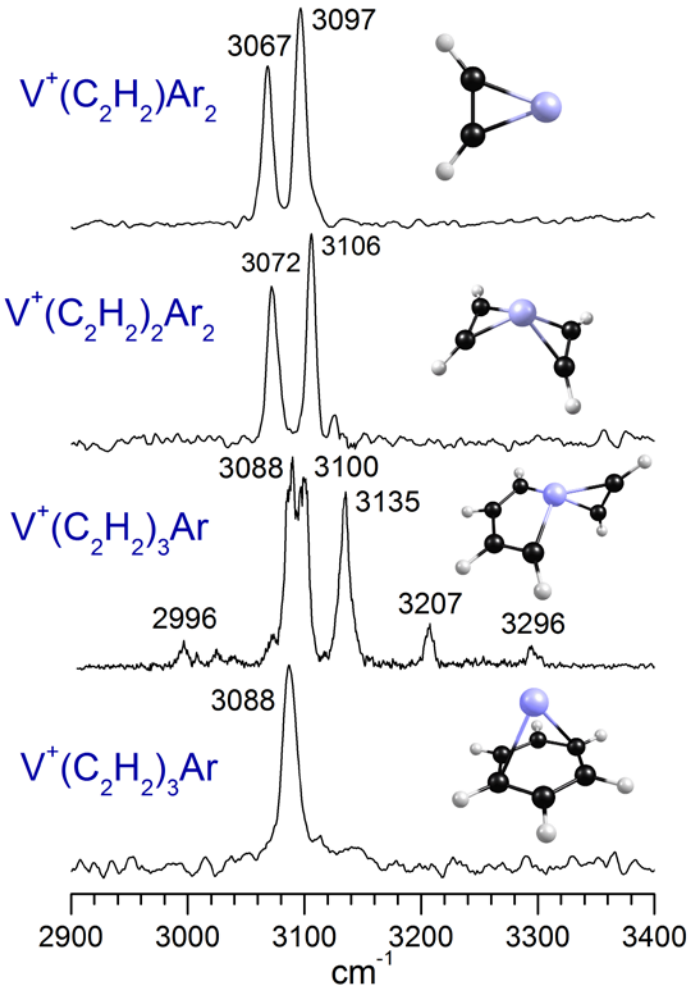

Figure x.13. The infrared spectra and structures formed from the addition of multiple acetylene ligands around vanadium ions. The third trace down shows the spectrum for $V^+(C_2H_2)$ at low concentration, while the bottom trace shows the same mass ion when acetylene is added at higher concentration. Cyclization chemistry occurs, which eventually forms benzene.

acetylenes bound in a three-membered ring metallacycle like that seen for the mono-acetylene complex. When three acetylenes are added, the spectrum becomes more complex, with several more vibrational bands spread over a wider frequency region. Additionally, the spectrum varies with the concentration of acetylene added to the experiment. The third trace down in the figure shows the spectrum measured at lower acetylene concentration (2.5% in argon), while the lower trace shows the spectrum measured with higher concentration (15%). The multi-band spectrum at lower concentration can be assigned to two isomers, primarily the one shown with both three- and five-membered metallacycle rings, and a secondary one with three, three-membered metallacycle rings. The single band in the lower spectrum is assigned to the V^+(benzene) complex! This is predicted by theory, which shows that this isomer is the most stable for this

composition, and it can also be confirmed by producing the same mass ion directly from benzene and measuring its spectrum, which is identical to that shown here. The structures mentioned for the spectrum of $V^+(C_2H_2)_3$ at low concentration have been implicated in previous theoretical work on other metal-acetylene systems as intermediates along the reaction path to form benzene via the cyclization of acetylene. Apparently, we have observed this same kind of cyclization chemistry here for the vanadium cation system. Although the cyclization of acetylene to form benzene is known chemistry on a number of different catalysts, the mechanism for the reaction has always been uncertain. Our infrared spectra at low concentration reveal for the first time the specific intermediate structures involved. Additional work will be necessary to understand the concentration dependence in more detail and to determine whether or not other metal ions might catalyze similar cyclization chemistry.

x.6. Metal-Benzene Complexes

Metal-benzene complexes are known for the formation of sandwiches, and cation-π interactions are well-studied in organometallic chemistry [6-11,16,280-283]. These systems have been studied in gas phase ion chemistry and with computational chemistry [290-307]. As shown in previous studies in our lab, the interaction of metal cations with the aromatic π system has distinctive effects on vibrational spectra. Charge transfer from the ring system toward the metal induces a red shift on the in-plane carbon ring distortion, ν_{19} (1486 cm^{-1} in isolated benzene), while this also causes a blue shift in the out-of-plane hydrogen bend, ν_{11} (673 cm^{-1} in isolated benzene) [167,303]. We documented these patterns for several cation-benzene systems in work done at the FELIX free electron laser using infrared multiphoton photodissociation (IR-MPD) spectroscopy on the ions without tagging [201-203], as the cluster source available at that time did not allow sufficient cooling for the formation of rare gas adducts. Unfortunately, the conditions used for the IR-MPD process can cause significant power broadening in spectral lines and shifts to lower frequencies. Rare gas tagging has not yet been applied to transition metal-benzene complexes, except for spectra in the C–H stretching region [165,166]. The vibrations most sensitive to the metal-benzene charge transfer are in the fingerprint region, and therefore the details of this chemistry are yet to be revealed.

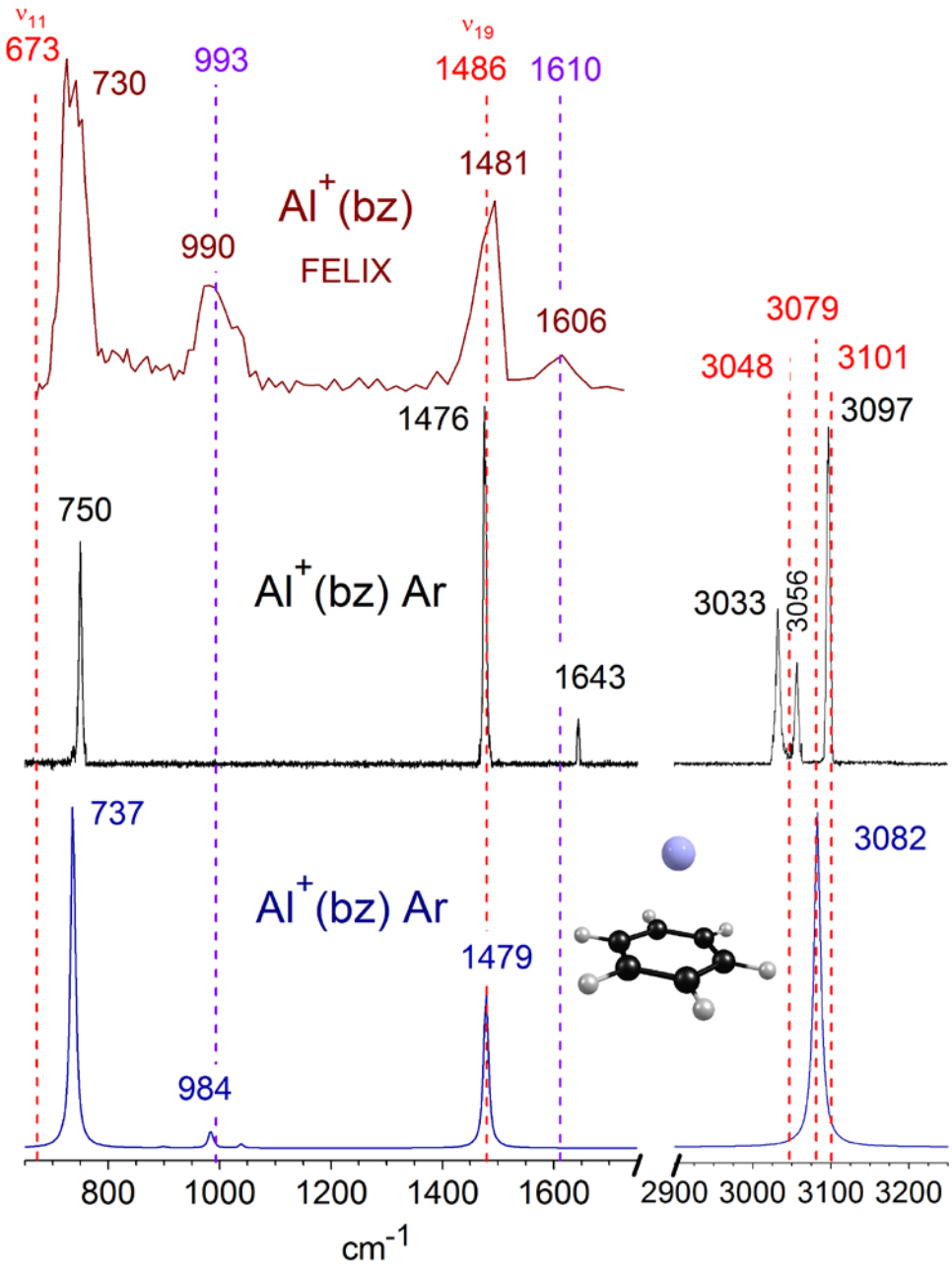

Figure x.14. The IR spectrum of Al^+(bz) in the C–H and fingerprint regions, measured with argon tagging (middle trace), compared to that measured with IR-MPD using the FELIX free electron laser (top trace). The lower trace shows the spectrum predicted by theory. The C–H stretch region has a triplet structure from a Fermi resonance, as seen in isolated benzene. Figure used from reference 168 with permission from the American Chemical Society, Copyright 2014.

The most well-studied metal ion-benzene complex is $Al^+(benzene)_n$, for which we have measured spectra for the n = 1–4 complexes using argon tagging [168]. The spectrum for the n = 1 complex is shown in Figure x.14, where it is compared to the spectrum reported previously for this

complex using IR-MPD with the FELIX free electron laser [202]. As shown, the quality of these tagged spectra is now far superior to the previous work in signal levels and resolution. Bands which were broad in the IR-MPD spectrum are much sharper, and the shifts from the IR-MPD process apparently occur in an unpredictable way to both higher and lower frequencies for different bands. The light red dashed lines in the figure show the positions of the free-benzene IR-active vibrations, including the well-known Fermi resonance that splits the single C–H stretch expected into a triplet [308]. The purple dashed lines show the positions of Raman-active (IR-inactive) vibrations, which appear in the IR spectrum of the metal ion complex because of its reduced symmetry. The red shift in the ν_{19} band associated with charge transfer is only 10 cm^{-1}, whereas the blue shift of the ν_{11} out-of-plane bending mode is 75 cm^{-1}. The former is much smaller than the shifts seen for transition metal complexes, consistent with their expected greater charge transfer, but the latter is comparable to the shifts seen before because it arises from the mechanical action of the bending hydrogens bumping into the metal. The data on the larger complexes reveals that the coordination around Al^+ contains *three* benzene molecules, i.e., it does not form the same kind of sandwich seen for transition metals. Clearly the quality of spectra for tagged ions is highly desirable, and our lab is working to get similar data for transition metal ion complexes. Ongoing work has obtained partial spectra for V^+(bz) and for $Co^+(bz)_2$ [309]. Both of these systems exhibit multiplet structure in the ν_{19} vibration, indicating that the benzene ring is distorted from its D_{6h} symmetric structure by the strong metal binding.

Although metal ion-benzene systems have been studied for many years, their electronic structure remains a significant challenge. In the case of V^+(benzene) and $V^+(benzene)_2$, ordinary DFT (B3LYP or BP86 functionals with large basis sets) misses the ground state spin configuration (triplet predicted; quintet agrees with experiment and higher level theory) [165,201]. Higher levels of theory get the correct quintet spin state for this system [305,306]. For $Ni^+(benzene)_2$, DFT apparently gets the wrong ground state structure (η^4 sandwich predicted; η^6 observed) [166]. As in the case for other systems, the 18-electron rule is a useful guiding principle for metal ion-benzene complexes. $Mn^+(benzene)_2$ is isoelectronic to the known neutral dibenzene chromium species, but the infrared spectrum of this ion has not yet been measured in the gas phase. Its expected η^6 coordination on the six-fold axis of benzene is common for many metal ions. However, later transition metal ions have more valence electrons, and do not need to interact with all six π electrons to achieve the 18-electron configuration. Some of these systems are known to adopt η^4 or lower

coordination in the condensed phase, and then their sandwich structures should have the two rings offset from each other. In extreme cases, some transition metals are predicted to bind strongly enough to distort the planarity of the ring (e.g., Fe^+, V^+, Co^+, Ni^+). All of these structures will lead to recognizable patterns in the fingerprint region. Future studies of these systems with tagging are therefore highly desirable.

A final aspect of these metal ion benzene complexes worth mentioning is that the early transition metal systems, particularly vanadium, form multiple decker sandwich structures with unusual electronic structure and bonding [297-299]. IR spectra have been obtained for neutrals following cation deposition on surfaces, but not for ions. These systems will be even more challenging for future experiments and theory.

x.7. Conclusions

The studies described in this chapter illustrate how infrared photodissociation spectroscopy can be applied to a variety of metal-molecular complexes in the gas phase. These gas phase studies eliminate the effects of solvent or counterions and make it possible to investigate isolated molecules with different numbers of ligand or solvent molecules. Vibrational band patterns, in coordination with computational predictions, make it possible to determine the structures of these complexes, and the effects that metal binding has on the geometry and charge distribution of the molecular adducts. Additionally, the spectral patterns reveal the number of ligand or solvent molecules making up the first (and sometimes higher) coordination sphere(s). In the case of carbonyl ligands, this provides an opportunity to make comparisons to several well-known neutral complexes that are isoelectronic analogs to the cations studied here. Because vibrational band patterns vary with the electronic state and spin multiplicity of the system, these spectra also make it possible to investigate the electronic structure of these complexes, and to identify strengths and weaknesses of density functional theory computations. We find examples in which DFT fails to describe the system adequately, such as the transition metal-benzene spin states, but also find many examples where it performs quite well to describe vibrational band patterns. The computations presented here usually employ the B3LYP functional. We have tried other functionals, especially including dispersion-corrected versions which are believed to describe the energetics of bonding more accurately. However, our experiments do not probe bonding energetics; they measure IR spectra. For this application, we find

that harmonic DFT/B3LYP calculations with proper scaling to account for anharmonicity provide the best description of vibrational patterns.

Although we have presented a variety of metal-molecular complexes here, there are clearly many more which could be investigated. Complexes with larger ligand or solvent molecules become more chemically interesting, and these studies can also be extended to metals other than the main group and transition metal species described here (e.g., lanthanides, actinides). We anticipate that this general area of activity will continue to provide fundamental insights into metal-molecular interactions for the foreseeable future.

Acknowledgements

This research was supported by the U. S. Department of Energy (grant no. DE-SC0018835), the National Science Foundation (grant no. CHE-1764111), and the Air Force Office of Scientific Research (grant no. FA-9550-15-1-0088).

References

1. Somorjai, G. A.: *Introduction to Surface Chemistry and Catalysis*, John Wiley & Sons, New York, 1994.
2. Henrich, V. E., Cox, P. A.: *The Surface Science of Metal Oxides*, Cambridge University Press, Cambridge, 1994.
3. Ertl, G.: *Reactions at Solid Surfaces*, John Wiley & Sons, Hoboken, NJ, 2009.
4. Ozin, G. A., Arsenault, A. C.: *Nanochemistry*, Royal Society of Chemistry Publishing, Cambridge, 2005.
5. Heiz, U., Landman, U., eds.: *Nanocatalysis*, Springer, Berlin, 2007.
6. van Leeuwen, P. W. N. M.: *Homogeneous Catalysis*, Kluwer, Dordrecht, 2004.
7. Hartwig, J. F.: *Organotransition Metal Chemistry: From Bonding to Catalysis*, University Science Books, Sausalito, CA, 2010.
8. Cotton, F. A., Wilkinson, G., Murillo, C.A., Bochmann, M.: *Advanced Inorganic Chemistry*, 6th ed., Wiley Interscience, New York, 1999.
9. Huhey, J. E., Keiter, E. A., Keiter, R. L.: *Inorganic Chemistry*, 4th ed., Harper Collins, New York, 1993.
10. Long, N. J.: *Metallocenes*, Blackwell Science, Oxford, U.K., 1998.
11. Crabtree, R. H.: *The Organometallic Chemistry of the Transition Metals*, 5th edition, John Wiley & Sons, Hoboken, N.J., 2009.
12. Burgess, J.: *Ions in Solution*, Horwood Publishing, Chichester, U.K., 1999.
13. Marcus, Y.: *Ion Solvation*, John Wiley & Sons, Chichester, U.K., 1985.
14. Richens, D. T. *The Chemistry of Aqua Ions*, John Wiley & Sons, Chichester, U. K., 1997.
15. Steed J. W., Atwood, J. L.: *Supramolecular Chemistry*, John Wiley and Sons, Chichester, U.K., 2009.
16. Bertini, I., Gray, H. B., Stiefel, E. I., Valentine, J. S.: *Biological Inorganic Chemistry*: *Structure and Reactivity*, University Science Books, Sausalito, CA, 2007.
17. Stoyanov, S. R., Titov, A. V., Král, P.: Transition metal and nitrogen doped carbon nanostructures. Coord. Chem. Rev. **253**, 2852–2871 (2009).
18. Kamat, P. V.: Graphene-based nanoarchitechtures. Anchoring semiconductor and metal nanoparticles on a two-dimensional carbon support. J. Phys. Chem. Lett. **1**, 520–527 (2010).
19. Lebedeva, M. A., Chamberlain, T. W., Khlobystov, A. N.: Harnessing the synergistic and complementary properties of fullerene and transition-metal compounds for nanomaterial applications. Chem. Rev. **115**, 11301–11351 (2015).
20. Low, J., Yu, J, Ho, W.: Graphene-based photocatalysts for CO_2 reduction to solar fuel. J. Phys. Chem. Lett. **6**, 4244–4251 (2015).
21. D'Alessandro, D. M., Smit, B., Long, J. R.: Carbon dioxide capture: Prospects for new materials. Angew. Chem. Int. Ed. **49**, 6058–6082 (2010).
22. Jena, P.: Materials for hydrogen storage: Past, present and future. J. Phys. Chem. Lett. **2**, 206–211 (2011).
23. Suh, M. P., Park, H. J., Prasad, T. K., Lim, D.-W.: Hydrogen storage in metal-organic frameworks. Chem. Rev. **112**, 782–835 (2012).
24. Yoon, M., Srirambalaji, R., Kim, K.: Homochiral metal-organic frameworks for asymmetric heterogeneous catalysis. Chem. Rev. **112**, 1196–1231 (2012).

25. Poloni, R., Lee, K., Berger, R. F., Smit, B., Neaton, J. B.: Understanding trends in CO_2 adsorption in metal-organic frameworks with open metal sites. J. Phys. Chem. Lett. **5**, 861–865 (2014).
26. Pera-Titus, M.: Porous inorganic membranes for CO_2 capture: Present and prospects. Chem. Rev. **114**, 1413–1492 (2014).
27. Gao, F., Goodman, D. W.: Model catalysts: Simulating the complexities of heterogeneous catalysts. Annu. Rev. Phys. Chem. **63**, 265–286 (2012).
28. Häkkinen, H.: Atomic and electronic structure of gold clusters: Understanding flakes, cages and superatoms from simple concepts. Chem. Soc. Rev. **37**, 1847–1859 (2008).
29. Lee, I., Albiter, M. A., Zhang, Q., Ge, J., Yin, Y., Zaera, F.: New nanostructured heterogeneous catalysts with increased selectivity and stability. Phys. Chem. Chem. Phys. **13**, 2449–2456 (2011).
30. Schauermann, S., Nilius, N., Shaikhutdinov, S., Freund, H.-J.: Nanoparticles for heterogeneous catalysis: New mechanistic insights. Acc. Chem. Res. **46**, 1673–1681 (2013).
31. McFarland, E. W., Metiu, H.: Catalysis by doped oxides. Chem. Rev. **113**, 4391–4427 (2013).
32. Reichert, R., Jusys, Z., Behm, R. J.: Au/TiO_2 photo(electro)catalysis: The role of Au cocatalyst in photoelectrochemical water splitting and photocatalytic H_2 evolution. J. Phys. Chem. C **119**, 24750–24759 (2015).
33. Esswein, A. J., Nocera, D. G.: Hydrogen production by molecular photocatalysis. Chem. Rev. **107**, 4022–4047 (2007).
34. Kortlever, R., Shen, J., Schouten, K. J. P., Calle-Vallejo, F., Koper, M. T. M.: Catalysts and reaction pathways for the electrochemical reduction of carbon dioxide. J. Phys. Chem. Lett. **6**, 4073–4082 (2015).
35. White, J. L., Baruch, M. F., Pander, J. E., III, Hu, Y., Fortmeyer, I. C., Park, J. E., Zhang, T., Liao, K., Gu, J., Yan, Y., Shaw, T. W., Abelev, E., Bocarsly, A. B.: Light-driven heterogeneous reduction of carbon dioxide: Photocatalysis and photoelectrodes. Chem. Rev. **115**, 12888–12935 (2015).
36. Blakemore, J. D., Crabtree, R. H., Brudvig, G. W.: Molecular catalysts for water oxidation. Chem. Rev. **115**, 12974–13005 (2015).
37. Jungwirth, P., Tobias, D. J.: Specific ion effects at the air/water interface. Chem. Rev. **106**, 1259–1281 (2006).
38. Jungwirth, P., B. Winter: Ions at aqueous interfaces: From water surface to hydrated proteins. Annu. Rev. Phys. Chem. **59**, 343–366 (2008).
39. Kohagen, M., Pluhařová, E., Mason, P. E., Jungwirth, P.: Exploring ion-ion interactions in aqueous solutions by a combination of molecular dynamics and neutron scattering. J. Phys. Chem. Lett. **6**, 1563–1567 (2015).
40. Tielrooij, K. J., Garcia-Araez, N., Bonn, M., Bakker, H. J.: Cooperativity in ion hydration. Science **328**, 1006–1009 (2010).
41. Tobias, D. J., Stern, A. C., Baer, M. D., Levin, Y., Mundy, C. J.: Simulation and theory of ions at atmospherically relevant aqueous liquid-air interfaces. Annu. Rev. Phys. Chem. **64**, 339–359 (2013).
42. Chen, H., Ruckenstein, E.: Hydrated ions: From individual ions to ion pairs to ion clusters. J. Phys. Chem. B **119**, 12671–12676 (2015).

43. Kanjana, K., Courtin, B., MacConnel, A., Bartels, D. M.: Reactions of hexa-aquo transition metal ions with the hydrated electron up to 300ºC. J. Phys. Chem. A **119**, 11094−11104 (2015).
44. Eller, K., Schwarz, H.: Organometallic chemistry in the gas phase. Chem. Rev. **91**, 1121−1177 (1991).
45. Freiser, B. S., ed.: *Organometallic Ion Chemistry*, Kluwer, Dordrecht, 1996.
46. Armentrout, P. B., Baer, T.: Gas phase ion dynamics and chemistry. J. Phys. Chem. **100**, 12866–12877 (1996).
47. Rodgers, M. T., Armentrout, P. B.: Noncovalent metal-ligand bond energies as studied by threshold collision-induced dissociation. Mass Spectrom. Rev. **19**, 215–247 (2000).
48. Armentrout, P. B.: Reactions and thermochemistry of small transition metal cluster ions. Ann. Rev. Phys. Chem. **52**, 423–461 (2001).
49. Ervin, K. M.: Metal-ligand interactions: Gas phase transition metal carbonyls. Int. Rev. Phys. Chem. **20**, 127−164 (2001).
50. Armentrout, P. B.: Guided ion beam studies of transition metal-ligand thermochemistry. Int. J. Mass Spectrom. **227**, 289−302 (2003).
51. Bohme, D. K., Schwarz, H.: Gas-phase catalysis by atomic and cluster metal ions: The ultimate single-site catalysts. Angew. Chem. Int. Ed. **44**, 2336–2354 (2005).
52. Operti, L., Rabezzana, R.: Gas phase ion chemistry in organometallic systems. Mass Spectrom. Rev. **25**, 483–513 (2006).
53. Roithova, J., Schröder, D.: Selective activation of alkanes by gas phase metal ions. Chem. Rev. **110**. 1170–1211 (2010).
54. Armentrout, P. B.: Fifty years of ion and neutral thermochemistry by mass spectrometry. Int. J. Mass Spectrometry **377**, 54–63 (2015).
55. Rodgers, M. T., Armentrout, P. B.: Cationic noncovalent interactions: Energetics and periodic trends. Chem. Rev. **116**, 5642–5678 (2016).
56. Ricca, A., Bauschlicher, C. W., Jr., Rosi, M.: Second-order Moller-Plesset perturbation theory for systems involving first transition row metals. J. Phys. Chem. **98**, 9498–9502 (1994).
57. Bauschlicher, C. W., Jr., Partridge, H., Langhoff, S. R.: The calculation of accurate metal-ligand bond energies. Adv. Met. Semicond. Clusters **2**, 165–202 (1994).
58. Nakamoto, K.: *Infrared and Raman Spectra of Inorganic and Coordination Compounds*, Parts A and B, 5th ed., John Wiley & Sons, New York, 1997.
59. Yates, J. T., Madey, T. E.: *Vibrational Spectroscopy of Molecules on Surfaces*, Plenum, New York, 1987.
60. Lessen, D. E., Asher, R. L., Brucat, P. J.: Cluster ion photodissociation spectroscopy. Adv. Metal & Semiconductor Clusters **1**, 267–302 (1993).
61. Asher, R. L., Bellert, D., Buthelezi, T., Brucat, P. J.: Optical Excitation of Co^+N_2. J. Phys. Chem. **99**, 1068–1072 (1995).
62. Hayes, T., Bellert, D., Buthelezi, T., Brucat, P. J.: The photodissociation of V^+-CH_4. Chem. Phys. Lett. **264**, 220–224 (1997).
63. Bellert, D., Buthelezi, T., Brucat, P. J.: The structure of Co^+-CO_2. Chem. Phys. Lett. **290**, 316–322 (1998).
64. Willey, K. F., Yeh, C. S., Robbins, D. L., Pilgrim, J. S., Duncan, M. A.: Photodissociation spectroscopy of Mg^+-H_2O and Mg^+-D_2O. J. Chem. Phys. **97**, 8886–8895 (1992).

65. Yeh, C. S., Willey, K. F., Robbins, D. L., Pilgrim, J. S., Duncan, M. A.: Photodissociation spectroscopy of the Mg^+-CO_2 complex and its isotopic analogs. J. Chem. Phys. **98**, 1867–1875 (1993).
66. Scurlock, C. T., Pullins, S. H., Reddic, J. E., Duncan, M. A.: Photodissociation spectroscopy of Ca^+-H_2O and Ca^+-D_2O. J. Chem. Phys. **104**, 4591–4599 (1996).
67. Scurlock, C. T., Pullins, S. H., Duncan, M. A.: Photodissociation spectroscopy of Ca^+-CO_2. J. Chem. Phys. **105**, 3579–3585 (1996).
68. Pullins, S. H., Reddic, J. E., France, M. R., Duncan, M. A.: Photodissociation spectroscopy of Ca^+-N_2. J. Chem. Phys. **108**, 2725–2732 (1998).
69. France, M. R., Pullins, S. H., Duncan, M. A.: Photodissociation Spectroscopy of Ca^+-C_2H_2 and Ca^+-C_2D_2 π-Complexes. J. Chem. Phys. **109**, 8842–8850 (1998).
70. Duncan, M. A.: Spectroscopy of metal ion complexes: Gas phase models for solvation. Ann. Rev. Phys. Chem. **48**, 63–93 (1997).
71. Farrar, J. M.: Size-dependent reactivity in open shell metal-ion polar solvent clusters: Spectroscopic probes of electronic-vibration coupling, oxidation and ionization. Int. Rev. Phys. Chem. **22**, 593–640 (2003).
72. Sanekata, M., Misaizu, F., Fuke, K.: Photodissociation study on $Ca^+(H_2O)_n$, n = 1–6: Electron structure and photoinduced dehydrogenation reaction. J. Chem. Phys. **104**, 9768–9778 (1996).
73. Misaizu, F., Sanekata, M., Tsukamoto, K., Fuke, K., Iwata, S.: Photodissociation of size-selected aquamagnesium ($Mg^+(H_2O)_n$) ions for n = 1 and 2. J. Phys. Chem. **96**, 8259–8264 (1992).
74. Chen, J., Wong, T. H., Cheng, Y. C., Montgomery, K., Kleiber, P. D.: Photodissociation spectroscopy and dynamics of $MgC_2H_4^+$. J. Chem. Phys. **108**, 2285–2296 (1998).
75. Chen, J., Wong, T. H., Kleiber, P. D., Wang, K. H.: Photofragmentation spectroscopy of $Al^+(C_2H_4)$. J. Chem. Phys. **110**, 11798–11805 (1999).
76. Abate, Y., Kleiber, P. D.: Photodissociation spectroscopy of $Zn^+(H_2O)$ and $Zn^+(D_2O)$. J. Chem. Phys. **122**, 084305 (2005).
77. Metz, R. B.: Photofragment spectroscopy of covalently bound transition metal complexes: A window into C-H and C-C bond activation by transition metal ions. Int. Rev. Phys. Chem. **23**, 79–108 (2004).
78. Metz, R. B.: Optical spectroscopy and photodissociation dynamics of multiply charged ions. Int. J. Mass Spectrom. **235**, 131–143 (2004).
79. Stringer, K. L., Citir, M., Metz, R. B.: Photofragment spectroscopy of π complexes: $Au^+(C_2H_4)$ and $Pt^+(C_2H_4)$. J. Phys. Chem. A **108**, 6996–7002 (2004).
80. Thompson, C. J., Faherty, K. P., Stringer, K. L., Metz, R. B.: Electronic spectroscopy and photodissociation dynamics of Co^{2+}-methanol clusters: $Co^{2+}(CH_3OH)_n$ (n=4–7). Phys. Chem. Chem. Phys. **7**, 814–818 (2005).
81. Cox, H., Stace, A. J.: Recent advances in the visible and UV spectroscopy of metal dication complexes. Int. Rev. Phys. Chem. **29**, 555–588 (2010).
82. Engelking, P. C., Lineberger, W. C.: Laser photoelectron spectrometry of the negative ions of iron and iron carbonyls. Electron affinity determination for the series $Fe(CO)_n$, n = 0,1,2,3,4. J. Am. Chem. Soc. **101**, 5569–5573 (1979).
83. Stevens, A. E., Feigerle, C. S., Lineberger, W. C.: Laser photoelectron spectrometry of $Ni(CO)_n^-$, n = 1–3. J. Am. Chem. Soc. **104**, 5026–5031 (1982).

84. Rathbone, G. J., Sanford, T., Andrews, D., Lineberger, W. C.: Photoelectron imaging spectroscopy of $Cu^{-}(H_2O)_{1,2}$ anion complexes. Chem. Phys. Lett. **401**, 570–574 (2005).
85. Bengali, A. A., Casey, S. M., Cheng, C. L., Dick, J. P., Fenn, P. T., Villalta, P. W., Leopold, D. G.: Negative ion photoelectron spectroscopy of coordinatively unsaturated group VI metal carbonyls: $Cr(CO)_3$, $Mo(CO)_3$ and $W(CO)_3$. J. Am. Chem. Soc. **114**, 5257–5268 (1992).
86. Miller, S. R., Marcy, T. P., Millam, E. L., Leopold, D. G.: Photoelectron spectroscopic characterization of the niobium-benzene anion produced by reaction of niobium with ethylene. J. Am. Chem. Soc. **129**, 3482–3483 (2007).
87. Klopcic, S. A., Moravec, V. D., Jarrold, C. C.: Anion photoelectron spectroscopy of $PdCO^{-}$ and $PdCN^{-}$: Reactivity of Pd^{-}. J. Chem. Phys. **110**, 8986–8991 (1999).
88. Moravec, V. D., Jarrold, C. C.: The electronic structure of PdC_2H and PdC_2HN determined by anion photoelectron spectroscopy. J. Chem. Phys. **112**, 792–798 (2000).
89. Judai, K., Hirano, M., Kawamata, H., Yabushita, S., Nakajima, A., Kaya, K.: Formation of vanadium-arene complex anions and their photoelectron spectroscopy. Chem. Phys. Lett. **270**, 23–30 (1997).
90. Masabuchi, T., Ohi, K., Iwasa, T., Nakajima, A.: Experimental and theoretical studies on the electronic properties of vanadium-benzene sandwich cluster anions, $V_nBz_{n+1}^{-}$ (n=1–5). J. Chem. Phys. **137**, 224305 (2012).
91. Gerhards, M., Thomas, O. C., Nilles, J. M., Zheng, W.-J., Bowen, K. H., Jr.: Cobalt-benzene cluster anions: Mass spectrometry and negative ion photoelectron spectroscopy. J. Chem. Phys. **116**, 10247–10252 (2002).
92. Zheng, W., Nilles, J. M., Thomas, O. C., Bowen, K. H., Jr.: Photoelectron spectroscopy of nickel-benzene cluster anions. J. Chem. Phys. **122**, 044306 (2005).
93. Zheng, W., Nilles, J. M., Thomas, O. C., Bowen, K. H., Jr.: Photoelectron spectroscopy of titanium-benzene cluster anions. Chem. Phys. Lett. **401**, 266–270 (2005).
94. Zheng, W., Eustis, S. N., Li, X., Nilles, J. M., Thomas, O. C., Bowen, K. H., Jr., Kandalam, A. K.: Photoelectron spectroscopic study of iron-benzene cluster anions. Chem. Phys. Lett. **462**, 35–39 (2008).
95. Zhang, X., Lim, E., Kim, S. K., Bowen, K. H., Jr.: Photoelectron spectroscopic and computational study of $(M\text{-}CO_2)^{-}$ anions, M = Cu, Ag, Au. J. Chem. Phys. **143**, 174305 (2015).
96. Yang, D.-S.: Zero electron kinetic energy photoelectron spectra of metal clusters and complexes. Adv. Metal Semiconductor Clusters **5**, 187–225 (2001).
97. Yang, D.-S.: High resolution electron spectroscopy of gas phase metal-aromatic complexes. J. Phys. Chem. Lett. **2**, 25–33 (2011).
98. Zhou, M., Andrews, L., Bauschlicher, C. W., Jr.: Spectroscopic and theoretical investigations of vibrational frequencies in binary unsaturated transition metal carbonyl cations, neutrals and anions. Chem. Rev. **101**, 1931–1962 (2001).
99. Okumura, M., Yeh, L. I., Lee, Y. T.: The vibrational predissociation spectroscopy of hydrogen cluster ions. J. Chem. Phys. **83**, 3705–3706 (1985).
100. Okumura, M., Yeh, L. I., Meyers, J. D., Lee, Y. T.: Infrared spectra of the cluster ions triaquahydrogen(1^{+})-molecular hydrogen ($H_7O_3^{+}\cdot H_2$) and tetraaquahydrogen(1^{+})-molecular hydrogen ($H_9O_4^{+}\cdot H_2$). J. Chem. Phys. **85**, 2328–2329 (1986).

101. Okumura, M., Yeh, L. I., Meyers, J. D., Lee, Y. T.: Infrared spectra of the solvated hydronium ion: vibrational predissociation spectroscopy of mass-selected $H_3O^+ \cdot (H_2O)_n \cdot (H_2)_m$. J. Phys. Chem. **94**, 3416–3427 (1990).
102. Lisy, J. M.: Spectroscopy and structure of solvated alkali-metal ions. Int. Rev. Phys. Chem. **16**, 267–289 (1997).
103. Ebata, T., Fujii, A., Mikami, N.: Vibrational spectroscopy of small-sized hydrogen-bonded clusters and their ions. Int. Rev. Phys. Chem. **17**, 331–361 (1998).
104. Wang, L.-S., Ding, C. F., Wang, X. B., Barlow, S. E.: Photodetachment photoelectron spectroscopy of multiply charged anions using electrospray ionization. Rev. Sci. Instrum. **70**, 1957–1966 (1999).
105. Bieske, E. J., Dopfer, O.: High resolution spectroscopy of cluster ions. Chem. Rev. **100**, 3963–3998 (2000).
106. Duncan, M. A.: Infrared spectroscopy to probe structure and dynamics in metal ion-molecule complexes. Int. Rev. Phys. Chem. **22**, 407–435 (2003).
107. Duncan, M. A.: Frontiers in the spectroscopy of mass-selected molecular ions. Int. J. Mass Spectrom. **200**, 545–569 (2000).
108. Robertson, W. H., Johnson, M. A.: Molecular aspects of halide ion hydration: The cluster approach. Annu. Rev. Phys. Chem. **54**, 173–213 (2003).
109. Rizzo, T. R., Stearns, J. A., Boyarkin, O. V.: Spectroscopic studies of cold, gas-phase biomolecular ions. Int. Rev. Phys. Chem. **28**, 481–515 (2009).
110. Baer, T., Dunbar, R. C.: Ion spectroscopy: Where did it come from; Where is it now; and Where is it going? J. Am. Soc. Mass Spectrom. **21**, 681–693 (2010).
111. Duncan, M. A.: Infrared laser spectroscopy of mass-selected carbocations. J. Phys. Chem. A **116**, 11477–11491 (2012).
112. Wolk, A. B., Leavitt, C. M., Garand, E., Johnson, M. A.: Cryogenic ion chemistry and spectroscopy. Acc. Chem. Res. **47**, 202–210 (2014).
113. Hock, C., Kim, J. B., Weichman, M. L., Yacovitch, T. I., Neumark, D. M.: Slow photoelectron velocity-map imaging spectroscopy of cold negative ions. J. Chem. Phys. **137**, 224201 (2012).
114. Redwine, J. G., Davis, Z. A., Burke, N. L., Oglesbee, R. A., McLuckey, S. A., Zwier, T. S.: A novel ion trap based tandem mass spectrometer for the spectroscopic study of cold gas phase polyatomic ions. Int. J. Mass Spectrom. **348**, 9–14 (2013).
115. Chakrabarty, S., Holtz, M., Campbell, E. K., Banerjee, A., Gerlich, D., Maier, J. P.: A novel method to measure electronic spectra of cold molecular ions. J. Phys. Chem. Lett. **4**, 4051–4054 (2013).
116. Duffy, E. M., Marsh, B. M., Garand, E.: Probing the hydrogen-bonded water network at the active site of a water oxidation catalyst: $Ru(bpy)(tpy)(H_2O)_2^+ \cdot (H_2O)_{0\text{-}4}$. J. Phys. Chem. A **119**, 6326–6332 (2015).
117. Heine, N., Asmis, K. R.: Cryogenic ion trap vibrational spectroscopy of hydrogen-bonded clusters relevant to atmospheric chemistry. Int. Rev. Phys. Chem. **34**, 1–34 (2015).
118. Roithová, J., Gray, A., Andris, E., Jašík, J., Gerlich, D.: Helium tagging infrared photodissociation spectroscopy of reactive ions. Acc. Chem. Res. **49**, 223–230 (2016).
119. Bosenberg, W. R., Guyer, D. R.: Broadly tunable, single-frequency optical parametric frequency-conversion system. J. Opt. Soc. Am. B **10**, 1716–1722 (1993).
120. Gerhards, M.: High energy and narrow bandwidth mid IR nanosecond laser system. Opt. Commun. **241**, 493–497 (2004).

121. Duncan, M. A.: Laser vaporization cluster sources. Rev. Sci. Instrum. **83**, 041101 (2012).
122. Cornett, D. S., Peschke, M., LaiHing, K., Cheng, P. Y., Willey, K. F., Duncan, M. A.: A reflectron time-of-flight mass spectrometer for laser photodissociation. Rev. Sci. Instrum. **63**, 2177–2186 (1992).
123. Gregoire, G., Duncan, M. A.: Infrared spectroscopy to probe structure and growth dynamics in $Fe^+(CO_2)_n$ complexes. J. Chem. Phys. **117**, 2120–2130 (2002).
124. Gregoire, G., Brinkman, N., Schaefer, H. F., Duncan, M. A.: Infrared photodissociation spectroscopy of $Mg^+(CO_2)_n$ and $Mg^+(CO_2)_nAr_m$ complexes. J. Phys. Chem. A **107**, 218–227 (2003).
125. Walters, R. S., Jaeger, T. D., Brinkman, N., Schaefer, H. F., Duncan, M. A.: Infrared photodissociation spectroscopy of $Al^+(CO_2)_n$ and $Al^+(CO_2)_nAr_m$ complexes. J. Phys. Chem. A **107**, 7396–7405 (2003).
126. Walker, N. R., Grieves, G. A., Walters, R. S., Duncan, M. A.: Growth dynamics and intracluster reactions in $Ni^+(CO_2)_n$ complexes via infrared spectroscopy. J. Chem. Phys. **121**, 10498–10507 (2004).
127. Walker, N. R., Walters, R. S., Duncan, M. A.: Infrared photodissociation spectroscopy of $V^+(CO_2)_n$ and $V^+(CO_2)_nAr$ complexes. J. Chem. Phys. **120**, 10037–10045 (2004).
128. Ricks, A. M., Brathwaite, A. D., Duncan, M. A.: IR spectroscopy of $V^+(CO_2)_n$ clusters: Solvation-induced electron transfer and activation of CO_2. J. Phys. Chem. A **117**, 11490–11498 (2013).
129. Walters, R. S., Walker, N. R., Pillai, E. D., Duncan, M. A.: Infrared spectroscopy of $V^+(H_2O)$ and $V^+(D_2O)$ complexes: Ligand deformation and an incipient reaction. J. Chem. Phys. **119**, 10471–10474 (2003).
130. Walters, R. S., Duncan, M. A.: Infrared spectroscopy of solvation and isomers in $Fe^+(H_2O)_{1,2}Ar_m$ complexes. Austr. J. Chem. **57**, 1145–1148 (2004).
131. Walker, N. R., Walters, R. S., Tsai, C.-S., Jordan, K. D., Duncan, M. A.: Infrared photodissociation spectroscopy of $Mg^+(H_2O)Ar_n$ complexes: Isomers in progressive microsolvation. J. Phys. Chem. A **109**, 7057–7067 (2005).
132. Walters, R. S., Pillai, E. D., Duncan, M. A.: Solvation processes in $Ni^+(H_2O)_n$ complexes revealed by infrared photodissociation spectroscopy. J. Am. Chem. Soc. **127**, 16599–16610 (2005).
133. Vaden, T. D., Lisy, J. M., Carnegie, P. D., Pillai, E. D., Duncan, M. A.: Infrared spectroscopy of the $Li^+(H_2O)Ar$ complex: The role of internal energy and its dependence on ion preparation. Phys. Chem. Chem. Phys. **8**, 3078–3082 (2006).
134. Kasalova, V., Allen, W. D., Schaefer, H. F., Pillai, E. D., Duncan, M. A.: Model systems for probing metal cation hydration: The $V^+(H_2O)$ and $V^+(H_2O)Ar$ complexes. J. Phys. Chem. A **111**, 7599–7610 (2007).
135. Carnegie, P. D., Bandyopadhyay, B., Duncan, M. A.: Infrared spectroscopy of $Cr^+(H_2O)$ and $Cr^{2+}(H_2O)$: The role of charge in cation hydration. J. Phys. Chem. A **112**, 6237–6243 (2008).
136. Carnegie, P. D., McCoy, A. B., Duncan, M. A.: Infrared spectroscopy and theory of $Cu^+(H_2O)Ar_2$ and $Cu^+(D_2O)Ar_2$: Fundamentals and combination bands. J. Phys. Chem. A **113**, 4849–4854 (2009).
137. Carnegie, P. D., Bandyopadhyay, B., Duncan, M. A.: Infrared spectroscopy of $Sc^+(H_2O)$ and $Sc^{2+}(H_2O)$ via argon complex predissociation: The charge dependence of cation hydration. J. Chem. Phys. **134**, 014302 (2011).

138. Bandyopadhyay, B., Carnegie, P. D., Duncan, M. A.: Infrared spectroscopy of $Mn^+(H_2O)_n$ and $Mn^{2+}(H_2O)$ complexes via argon complex predissociation. J. Phys. Chem. A **115**, 7602–7609 (2011).
139. Bandyopadhyay, B., Duncan, M. A.: Infrared spectroscopy of $V^{2+}(H_2O)$ complexes. Chem. Phys. Lett. **530**, 10–15 (2012).
140. Bandyopadhyay, B., Reishus, K. N., Duncan, M. A.: Infrared spectroscopy of solvation in small $Zn^+(H_2O)_n$ complexes. J. Phys. Chem. A **117**, 7794–7803 (2013).
141. Ward, T. B., Carnegie, P. D., Duncan, M. A.: Infrared spectroscopy of the $Ti(H_2O)Ar^+$ ion-molecule complex: Electronic state switching induced by argon. Chem. Phys. Lett. **654**, 1–5 (2016).
142. Ward, T. B., Miliordos, E., Carnegie, P. D., Xantheas, S. S., Duncan, M. A.: Ortho-para interconversion in cation-water complexes: The case of $V^+(H_2O)$ and $Nb^+(H_2O)$ clusters. J. Chem. Phys. **146**, 224305 (2017).
143. Velasquez, J., III, Njegic, B., Gordon, M. S., Duncan, M. A.: IR photodissociation spectroscopy and theory of $Au^+(CO)_n$ complexes: Nonclassical carbonyls in the gas phase. J. Phys. Chem. A **112**, 1907–1913 (2008).
144. Velasquez, J., III, Duncan, M. A.: IR photodissociation spectroscopy of $Pt^+(CO)_n$ complexes. Chem. Phys. Lett. **461**, 28–32 (2008).
145. Ricks, A. M., Bakker, J. M., Douberly, G. E., Duncan, M. A.: IR spectroscopy of $Co^+(CO)_n$ complexes in the gas phase. J. Phys. Chem. A **113**, 4701–4708 (2009).
146. Ricks, A. M., Reed, Z. D., Duncan, M. A.: Seven-coordinate homoleptic metal carbonyls in the gas phase. J. Am. Chem. Soc. **131**, 9176–9177 (2009).
147. Reed, Z. D., Duncan, M. A.: Infrared spectroscopy and structures of manganese carbonyl cations, $Mn(CO)_n^+$ (n = 1–9). J. Am. Soc. Mass Spectrom. **21**, 739–749 (2010).
148. Ricks, A. M., Gagliardi, L., Duncan, M. A.: Infrared spectroscopy of extreme coordination: The carbonyls of U^+ and UO_2^+. J. Am. Chem. Soc. **132**, 15905–15907 (2010).
149. Ricks, A. M., Reed, Z. D., Duncan, M. A.: IR spectroscopy of gas phase metal carbonyl cations. J. Mol. Spec. **266**, 63–74 (2011).
150. Brathwaite, A. D., Reed, Z. D., Duncan, M. A.: Infrared spectroscopy of copper carbonyl cations. J. Phys. Chem. A **115**, 10461–10469 (2011).
151. Ricks, A. M., Brathwaite, A. D., Duncan, M. A.: Coordination and spin states of $V^+(CO)_n$ clusters revealed by IR spectroscopy. J. Phys. Chem. A **117**, 1001–1010 (2013).
152. Brathwaite, A. D., Duncan, M. A.: Infrared photodissociation spectroscopy of saturated group IV (Ti, Zr, Hf) metal carbonyl cations. J. Phys. Chem. A **117**, 11695–11703 (2013).
153. Brathwaite, A. D., Ricks, A. M., Duncan, M. A.: Infrared spectroscopy of vanadium oxide carbonyl cations. J. Phys. Chem. A **117**, 13435–13442 (2013).
154. Brathwaite, A. D., Maner, J. A., Duncan, M. A.: Testing the limits of the 18-electron rule: The gas phase carbonyls of Sc^+ and Y^+. Inorg. Chem. **53**, 1166–1169 (2014).
155. Brathwaite, A. D., Abbott-Lyon, H. L., Duncan, M. A.: Distinctive coordination of CO vs N_2 to rhodium cations: An infrared and computational study. J. Phys. Chem. A **120**, 7659–7670 (2016).
156. Walters, R. S., Jaeger, T. D., Duncan, M. A.: Infrared spectroscopy of $Ni^+(C_2H_2)_n$ complexes: Evidence for intracluster cyclization reactions. J. Phys. Chem. A **106**, 10482–10487 (2002).

157. Walters, R. S., Schleyer, P. v. R., Corminboeuf, C., Duncan, M. A.: Structural trends in transition metal cation-acetylene complexes revealed through the C–H stretch fundamentals. J. Am. Chem. Soc. **127**, 1100–1101 (2005).
158. Walters, R. S., Pillai, E. D., Schleyer, P. v. R., Duncan, M. A.: Vibrational spectroscopy of $Ni^+(C_2H_2)_n$ (n=1–4) complexes. J. Am. Chem. Soc. **127**, 17030–17042 (2005).
159. Brathwaite, A. D., Ward, T. B., Walters, R. S., Duncan, M. A.: Cation-π and CH-π interactions in the coordination and solvation of Cu^+(acetylene)$_n$ complexes. J. Phys. Chem. A **119**, 5658–5667 (2015).
160. Ward, T. B., Brathwaite, A. D., Duncan, M. A.: Infrared spectroscopy of $Au(Acetylene)_n^+$ complexes in the gas phase. Top. Catal. **61**, 49–61 (2018).
161. Marks, J. H., Ward, T. B., Duncan, M. A.: Infrared spectroscopy of the coordination and solvation in Cu^+(ethylene)$_n$ (n = 1–9) complexes. Int. J. Mass Spectrom. **435**, 107–113 (2019).
162. Ward, T. B., Marks, J. H., Brathwaite, A. D., Duncan, M. A.: Cyclotrimerization of acetylene in gas phase $V^+(C_2H_2)_n$ complexes detected with infrared spectroscopy. to be submitted.
163. Pillai, E. D., Jaeger, T. D., Duncan, M. A.: Infrared spectroscopy and density functional theory of small $V^+(N_2)_n$ clusters. J. Phys. Chem. A **109**, 3521–3526 (2005).
164. Pillai, E. D., Jaeger, T. D., Duncan, M. A.: Infrared spectroscopy of $Nb^+(N_2)_n$ complexes: Coordination, structures and spin states. J. Am. Chem. Soc. **129**, 2297–2307 (2007).
165. Jaeger, T. D., Duncan, M. A.: Structure, coordination and solvation in V^+(benzene)$_n$ complexes via gas phase infrared spectroscopy. J. Phys. Chem. A **108**, 6605–6610 (2004).
166. Jaeger, T. D., Duncan, M. A.: Infrared photodissociation spectroscopy of Ni^+(benzene)$_x$ complexes. J. Phys. Chem. A **109**, 3311–3317 (2005).
167. Duncan, M. A.: Structures, energetics and spectroscopy of gas phase transition metal ion-benzene complexes. Int. J. Mass Spectrom. **272**, 99–118 (2008).
168. Reishus, K. N., Brathwaite, A. D., Mosley, J. D., Duncan, M. A.: Infrared spectroscopy of coordination versus solvation in Al^+(benzene)$_{1-4}$ complexes. J. Phys. Chem. A **118**, 7516−7525 (2014).
169. Inokuchi, Y., Ohshimo, K., Misaizu, F., Nishi, N.: Structures of $[Mg(H_2O)_{1,2}]^+$ and $[Al(H_2O)_{1,2}]^+$ ions studied by infrared photodissociation spectroscopy: Evidence of $[HO\text{-}Al\text{-}H]^+$ ion core structure in $[Al(H_2O)_2]^+$. Chem. Phys. Lett. **390**, 140–144 (2004).
170. Inokuchi, Y., Ohshimo, K., Misaizu, F., Nishi, N.: Infrared photodissociation spectroscopy of $[Mg(H_2O)_{1\text{-}4}]^+$ and $[Mg(H_2O)_{1\text{-}4}Ar]^+$. J. Phys. Chem. A **108**, 5034–5040 (2004).
171. Iino, T., Ohashi, K., Inoue, K., Judai, K., Nishi, N., Sekiya, H.: Infrared spectroscopy of $Cu^+(H_2O)_n$ and $Ag^+(H_2O)_n$: coordination and solvation of noble-metal ions. J. Chem. Phys. **126**, 194302 (2007).
172. Sasaki, J., Ohashi, K., Inoue, K., Imamura, T., Judai, K., Nishi, N., Sekiya, H.: Infrared photodissociation spectroscopy of $V^+(H_2O)_n$ (n = 2–8): Coordinative saturation of V^+ with four H_2O molecules. Chem. Phys. Lett. **474**, 36–40 (2009).
173. Furukawa, K., Ohashi, K., Koga, N., Imamura, T., Judai, K., Nishi, N., Sekiya, H.: Coordinatively unsaturated cobalt ion in $Co^+(H_2O)_n$ (n = 4–6) probed with infrared photodissociation spectroscopy. Chem. Phys. Lett. **508**, 202–206 (2011).
174. Weber, J. M.: The interaction of negative charge with carbon dioxide - insight into solvation, speciation and reductive activation from cluster studies. Int. Rev. Phys. Chem. **33**, 489–519 (2014).

175. Dodson, L. G., Thompson, M. C., Weber, J. M.: Characterization of intermediate oxidation states in CO_2 activation. Annu. Rev. Phys. Chem. **69**, 231–252 (2018).
176. Citir, M., Altinay, G., Metz, R. B.: Electronically and vibrational spectroscopy and vibrationally mediated photodissociation of $V^+(OCO)$. J. Phys. Chem. A **110**, 5051–5057 (2006).
177. Citir, M., Altinay, G., Austein-Miller, G., Metz, R. B.: Vibrational spectroscopy and theory of $Fe^+(CH_4)_n$ (n=1–4). J. Phys. Chem. A **114**, 11322–11329 (2010).
178. Daluz, J. S., Kocak, A., Metz, R. B.: Photodissociation studies of the electronic and vibrational spectroscopy of $Ni^+(H_2O)$. J. Phys. Chem. A **116**, 1344–1352 (2012).
179. Kocak, A., Austein-Miller, G., Pearson, W. L., III, Altinay, G., Metz, R. B.: Dissociation energy and electronic and vibrational spectroscopy of $Co^+(H_2O)$ and its isotopomers. J. Phys. Chem. A **117**, 1254–1264 (2013).
180. Kocak, A., Sallese, Z., Johnston, M. D., Metz, R. B.: Vibrational spectroscopy of $Co^+(CH_4)_n$ and $Ni^+(CH_4)_n$ (n = 1–4). J. Phys. Chem. A **118**, 3253–3265 (2014).
181. Pearson, W. L., III, Copeland, C., Kocak, A., Sallese, Z., Metz, R. B.: Near ultraviolet photodissociation spectroscopy of $Mn^+(H_2O)$ and $Mn^+(D_2O)$. J. Chem. Phys. **141**, 204305 (2014).
182. Kocak, A., Ashraf, M. A., Metz, R. B.: Vibrational spectroscopy reveals varying structural motifs in $Cu^+(CH_4)_n$ and $Ag^+(CH_4)_n$ (n = 1−6). J. Phys. Chem. A **119**, 9653–9665 (2015).
183. Bush, M. F., Saykally, R. J., Williams, E. R.: Hydration of the calcium dication: Direct evidence for second shell formation from infrared spectroscopy. ChemPhysChem **8**, 2245–2253 (2007).
184. O'Brien, J. T., Williams, E. R.: Hydration of gaseous copper dications probed by IR action spectroscopy. J. Phys. Chem. A **112**, 5893–5901 (2008).
185. Bush, M. F., Saykally, R. J., Williams, E. R.: Reactivity and infrared spectroscopy of gaseous hydrated trivalent metal ions. J. Am. Chem. Soc. **130**, 9122–9128 (2008).
186. Bush, M. F., O'Brien, J. T., Prell, J. S., Wu, C.-C., Saykally, R. J., Williams, E. R.: Hydration of alkaline earth metal dications: Effects of metal ion size determined using infrared action spectroscopy. J. Am. Chem. Soc. **131**, 13270–13277 (2009).
187. O'Brien, J. T., Williams, E. R.: Coordination numbers of hydrated divalent transition metal ions investigated with IRPD spectroscopy. J. Phys. Chem. A **115**, 14612–14619 (2011).
188. Dryza, V., Poad, B. L. J., Bieske, E. J.: Attaching molecular hydrogen to metal cations: Perspectives from gas-phase infrared spectroscopy. Phys. Chem. Chem. Phys. **14**, 14954–14965 (2012).
189. Dryza, V., Bieske, E. J.: Non-covalent interactions between metal cations and molecular hydrogen: Spectroscopic studies of M^+-H_2 complexes. Int. Rev. Phys. Chem. **32**, 559–587 (2013).
190. Wang, G., Chi, C., Cui, J., Xing, X., Zhou, M.: Infrared photodissociation spectroscopy of mononuclear iron carbonyl anions. J. Phys. Chem. A **116**, 2484–2489 (2012).
191. Chi, C., Cui, J., Xing, X., Wang, G., Zhou, M.: Infrared photodissociation spectroscopy of trigonal bipyramidal 19-electron $Ni(CO)_5^+$ cation. Chem. Phys. Lett. **542**, 33–36 (2012).
192. Li, Y., Wang, G., Wang, C., Zhou, M.: Coordination and solvation of the Au^+ cation: Infrared photodissociation spectroscopy of mass-selected $Au(H_2O)_n^+$ (n = 1–8) complexes. J. Phys. Chem. A **116**, 10793–10801 (2012).

193. Zhou, X., Cui, J., Li, Z. H., Wang, G., Zhou, M.: Infrared photodissociation spectroscopy and theoretical study of homoleptic dinuclear chromium carbonyl cluster cations with a linear bridging carbonyl group. J. Phys. Chem. A **116**, 12349–12356 (2012).
194. Wang, G., Cui, J., Cui, C., Zhou, X., Li, Z. H., Xing, X., Zhou, M.: Bonding in homoleptic iron carbonyl cluster cations: A combined infrared photodissociation and theoretical study. Chem. Sci. **3**, 3272–3279 (2012).
195. Zhou, X., Cui, J., Li, Z. H., Wang, G., Liu, Z., Zhou, M.: Carbonyl bonding on oxophilic metal centers: infrared photodissociation spectra of mononuclear and dinuclear titanium carbonyl cation complexes. J. Phys. Chem. A **117**, 1514–1521 (2013).
196. Jin, J., Yang, T., Xin, K., Wang, G., Jin, X., Zhou, M., Frenking, G.: Octacarbonyl anion complexes of group three transition metals $[TM(CO)_8]^-$ (TM = Sc, Y, La) and the 18-electron rule. Angew. Chem. Int. Ed. **57**, 6236–6241 (2018).
197. Wu, X., Zhao, L., Jin, J., Pan, S., Li, W., Jin, X., Wang, G., Zhou, M., Frenking, G.: Observation of alkaline earth complexes $M(CO)_8$ (M = Ca, Sr, or Ba) that mimic transition metals. Science **361**, 912–916 (2018).
198. Garand, E., Fournier, J. A., Kamrath, M. Z., Schley, N. D., Crabtree, R. H., Johnson, M. A.: Characterization of an activated iridium water splitting catalyst using infrared photodissociation of H_2 tagged ions. Phys. Chem. Chem. Phys. **14**, 10109–10113 (2012).
199. Johnson, C. J., Dzugan, L. C., Wolk, A. B., Leavitt, C. M., Fournier, J. A., McCoy, A. B., Johnson, M. A.: Microhydration of contact ion pairs in $M^{2+}OH^-(H_2O)_{n = 1\text{-}5}$ (M = Mg, Ca) clusters: Spectral manifestations of a mobile proton defect in the first hydration sphere. J. Phys. Chem. A **118**, 7590–7597 (2014).
200. DePalma, J. W., Kelleher, P. J., Johnson, C. J., Fournier, J. A., Johnson, M. A.: Vibrational signatures of solvent-mediated deformation of the ternary core ion in size-selected $[MgSO_4Mg(H_2O)_{n = 4\text{-}11}]^{2+}$ clusters. J. Phys. Chem. A **119**, 8294–8302 (2015).
201. van Heijnsbergen, D., von Helden, G., Meijer, G., Maître, P., Duncan, M. A.: Infrared spectroscopy of V^+(benzene) and V^+(benzene)$_2$ complexes in the gas phase. J. Am. Chem. Soc. **124**, 1562–1563 (2002).
202. van Heijnsbergen, D., Jaeger, T. D., von Helden, G., Meijer, G., Duncan, M. A.: Infrared spectroscopy of Al^+(benzene) in the gas phase. Chem. Phys. Lett. **364**, 345–351 (2002).
203. Jaeger, T. D., van Heijnsbergen, D., Klippenstein, S., von Helden, G., Meijer, G., Duncan, M. A.: Infrared spectroscopy and density functional theory of transition metal ion-benzene and dibenzene complexes. J. Am. Chem. Soc. **126**, 10981–10991 (2004).
204. Oomens, J., Moore, D. T., von Helden, G., Meijer, G., Dunbar, R. C.: The site of Cr^+ attachment to gas-phase aniline from infrared spectroscopy. J. Am. Chem. Soc. **126**, 724–725 (2004).
205. Moore, D. T., Oomens, J., Eyler, J. R., Meijer, G., von Helden, G., Ridge, D. P.: Gas-phase IR spectroscopy of anionic iron carbonyl clusters. J. Am. Chem. Soc. **126**, 14726–14727 (2004).
206. Fielicke, A., von Helden, G., Meijer, G., Petersen, D. B., Simard, B., Rayner, D. M.: Size and charge effects on the binding of CO to small isolated rhodium clusters. J. Phys. Chem. B **108**, 14591–14598 (2004).
207. Moore, D. T., Oomens, J., Eyler, J. R., von Helden, G., Meijer, G., Dunbar, R. C.: Infrared spectroscopy of gas phase Cr^+ coordination complexes: Determination of binding sites and electronic states. J. Am. Chem. Soc. **127**, 7243–7254 (2005).

208. Fielicke, A., von Helden, G., Meijer, G., Petersen, D. B., Simard, B., Rayner, D. M.: Size and charge effects on the binding of CO to late transition metal clusters. J. Chem. Phys. **124**, 194305 (2006).
209. Fielicke, A., von Helden, G., Meijer, G., Simard, B., Rayner, D. M.: Gold cluster carbonyls: Vibrational spectroscopy of the anions and the effects of cluster size, charge, and coverage on the CO stretching frequency. J. Phys. Chem. B **109**, 23935–23940 (2005).
210. Simon, A., Jones, W., Ortega, J.-M., Boissel, P., Lemaire, J., Maître, P.: Infrared multiphoton dissociation spectroscopy of gas-phase mass-selected hydrocarbon-Fe^+ complexes. J. Am. Chem. Soc. **126**, 11666–11674 (2004).
211. MacAleese, L., Maître, P.: Infrared spectroscopy of organometallic ions in the gas phase: from model to real world complexes. Mass Spectrom. Rev. **26**, 583–605 (2007).
212. Reinhard, B. M., Lagutschenkov, A., Lemaire, J., Maître, P., Boissel, P., Niedner-Schatteburg, G.: Reductive nitrile coupling in niobium-acetonitrile complexes probed by free electron laser multiphoton dissociation spectroscopy. J. Phys. Chem. A **108**, 3350–3355 (2004).
213. Harvey, J. N.: DFT computation of relative spin-state energetics of transition metal compounds. Structure and Bonding **112**,151–183 (2004).
214. Cramer, C. J., Truhlar, D. J.: Density functional theory for transition metals and transition metal chemistry. Phys. Chem. Chem. Phys. **11**, 10757–10816 (2009).
215. Li, S., Hennigan, J. M., Dixon, D. A., Peterson, K. A.: Accurate thermochemistry for transition metal oxide clusters. J. Phys. Chem. A **113**, 7861–7877 (2009).
216. Cohen, A. J., Mori-Sanchez, P., Yang, W.: Challenges for density functional theory. Chem. Rev. **112**, 289–320 (2012).
217. Ramabhadran, R. O., Becher, E. L., III, Chowdhury, A., Raghavachari, K.: Fluxionality in the chemical reactions of transition metal oxide clusters: The role of metal, spin state, and the reactant molecule. J. Phys. Chem. A **116**, 7189–7195 (2012).
218. Shil, S., Bhattacharya, D., Sarkar, S., Misra, A.: Performance of the widely used Minnesota density functionals for the prediction of heat of formations, ionization potentials of some benchmarked first row transition metal complexes. J. Phys. Chem. A **117**, 4945–4955 (2013).
219. Frenking, G., Fröhlich, N.: The nature of the bonding in transition-metal compounds. Chem. Rev. **100**, 717–774 (2000).
220. Huber , K. P., Herzberg, G.: *Constants of Diatomic Molecules*, Van Nostrand Reinhold, New York, 1979.
221. Khan, F. A., Clemmer, D. E., Schultz, R. H., Armentrout, P. B.: Sequential bond energies of chromium carbonyls ($Cr(CO)_x^+$, x = 1–6). J. Phys. Chem. **97**, 7978–7987 (1993).
222. Sievers, M. R., Armentrout, P. B.: Collision-induced dissociation studies of $V(CO)_x^+$, x = 1–7: Sequential bond energies and the heat of formation of $V(CO)_6$. J. Phys. Chem. **99**, 8135–8141 **(**1995).
223. Meyer, F., Chen, Y. M., Armentrout, P. B.: Sequential bond energies of $Cu(CO)_x^+$ and $Ag(CO)_x^+$ (x = 1–4). J. Am. Chem. Soc. **117**, 4071–4081 (1995).
224. Goebel, S., Haynes, C. L., Khan, F. A., Armentrout, P. B.: Collision-induced dissociation studies of $Co(CO)_x^+$, x = 1–5: Sequential bond energies and heats of formation of $Co(CO)_4$. J. Am. Chem. Soc. **117**, 6994–7002 (1995).
225. Meyer, F., Armentrout, P. B.: Sequential bond energies of $Ti(CO)_x^+$, x = 1–7. Mol. Phys. **88**, 187–197 (1996).

226. Zhang, X. G., Armentrout, P. B.: Sequential bond energies of $Pt(CO)_x^+$ (x = 1–4) determined by collision-induced dissociation. Organometallics **20**, 4266–4273 (2001).
227. Bauschlicher, C. W., Jr.: Transition metal-ligand bonding, II. J. Chem. Phys. **84**, 260–267 (1986).
228. Bauschlicher, C. W., Jr., Bagus, P. S., Nelin, C. J., Roos, B. J.: The nature of bonding in XCO for X=Fe, Ni and Cu. J. Chem. Phys. **85**, 354–364 (1986).
229. Bauschlicher, C. W., Jr., Barnes, L. A.: On the dissociation energies and bonding in $NiCO^+$ and $TiCO^+$. Chem. Phys. **124**, 383–394 (1988).
230. Barnes, L. A., Rosi, M., Bauschlicher, C. W., Jr.: Theoretical studies of the first- and second-row mono- and di-carbonyl positive ions. J. Chem. Phys. **93**, 609–624 (1990).
231. Sodupe, M., Bauschlicher, C. W., Jr., Lee, T. J.: The calculation of the vibrational frequencies of $CuCO^+$, NiCO and $CuCH_3$. Chem. Phys. Lett. **189**, 266–272 (1992).
232. Goldman, A. S., Krogh-Jespersen, K.: Why do cationic carbon monoxide complexes have high CO stretching force constants and short CO bonds? Electrostatic effects, not σ bonding. J. Am. Chem. Soc. **118**, 12159–12166 (1996).
233. Lupinetti, A. J., Fau, S., Frenking, G., Strauss, S. H.: Theoretical analysis of the bonding between CO and positively charged atoms. J. Phys. Chem. **101**, 9551–9559 (1997).
234. Lupinetti, A. J., Frenking, G., Strauss, S. H.: Nonclassical metal carbonyls. Angew. Chem. Int. Ed. **37**, 2113–2116 (1998).
235. Lupinetti, A. J., Strauss, S. H., Frenking, G.: Non-classical metal carbonyls. Prog. Inorg. Chem. **49**, 1–112 (2001).
236. O'Dwyer, M. F.: Infrared spectra and normal coordinate analysis of iron pentacarbonyl from vibrational spectra of isotopic species. J. Mol. Spec. **2**, 144– (1958).
237. Shufler, S. L., Sternberg, H. W., Friedel, R. A.: Infrared spectrum and structure of chromium hexacarbonyl, $Cr(CO)_6$. J. Am. Chem. Soc. **78**, 2687– (1956).
238. Boquet, G., Birgone, M.: Infrared spectra of $Ni(CO)_4$ in the gas phase. Spectrochim. Acta **27**, 139– (1971).
239. Ryther, R. J., Weitz, E.: Reaction kinetics of coordinatively unsaturated iron carbonyls formed on gas-phase excimer laser photolysis of iron pentacarbonyl. J. Phys. Chem. **95**, 9841–9852 (1991).
240. Weitz, E.: Transient infrared spectroscopy as a probe of coordinatively unsaturated metal carbonyls in the gas phase. J. Phys. Chem. **98**, 11256–11264 (1994).
241. Harvey, J. N., Aschi, M.: Modeling spin-forbidden reactions: Recombination of carbon monoxide with iron tetracarbonyl. Faraday Discuss. **124**, 129–143 (2003).
242. Besora, M., Carreón-Macedo, J.-L., Cimas, Á., Harvey, J. N.: Spin-state changes and reactivity in transition metal chemistry: Reactivity of iron tetracarbonyl. Adv. Inorg. Chem. **61**, 573–623 (2009).
243. Besora, M., Carreón-Macedo, J.-L., Cowan, A. J., George, M. W., Harvey, J. N., Portius, P., Ronayne, K. L., Sun, X.-Z., Towrie, M. A.: Combined theoretical and experimental study on the role of spin states in the chemistry of $Fe(CO)_5$ photoproducts. J. Am. Chem. Soc. **131**, 3583–3592 (2009).
244. Asmis, K. R., Sauer, J.: Mass-selective vibrational spectroscopy of vanadium oxide cluster ions. Mass Spectrom. Rev. **26**, 542–562 (2007).
245. Sodupe, M., Branchadell, V., Bauschlicher, C. W., Jr.: Theoretical study of M^+-CO_2 and OM^+CO systems for the first transition row metal atoms. J. Phys. Chem. A **101**, 7854–7859 (1997).

246. Sievers, M. R., Armentrout, P. B.: Activation of carbon dioxide: Gas-phase reactions of Y^+, YO^+ and YO_2^+ with CO and CO_2. Inorg. Chem. **38**, 397–402 (1999).
247. Armentrout, P. B., Koizumi, H., MacKenna, M.: Sequential bond energies of $Fe^+(CO_2)_n$, n = 1–5, determined by threshold collision-induced dissociation and ab initio theory. J. Phys. Chem. A **109**, 11365–11375 (2005).
248. Shimanouchi, T.: Molecular Vibrational Frequencies in *NIST Chemistry WebBook*, NIST Standard Reference Database Number 69, Eds. Linstrom, P. J., Mallard, W. H., National Institute of Standards and Technology, Gaithersburg MD, 20899 (http://webbook.nist.gov).
249. Marinelli, P. J., Squires, R. R.: Sequential solvation of atomic transition-metal ions. The second solvent molecule can bind more strongly than the first. J. Am. Chem. Soc. **111**, 4101–4103 (1989).
250. Dalleska, N. F., Honma, K., Sunderlin, L. S., Armentrout, P. B.: Solvation of transition metal ions by water. Sequential binding energies of $M^+(H_2O)_x$ (x = 1–4) for Ti to Cu determined by collision induced dissociation. J. Am. Chem. Soc. **116**, 3519–3528 (1994).
251. Rosi, M., Bauschlicher, C. W., Jr.: The binding energies of one and two water molecules to the first transition-row metal positive ions. J. Chem. Phys. **90**, 7264–7272 (1989).
252. Rosi, M., Bauschlicher, C. W., Jr.: The binding energies of one and two water molecules to the first transition-row metal positive ions II. J. Chem. Phys. **92**, 1876–1878 (1990).
253. Poisson, L., Pradel, P., Lepetit, F., Reau, F., Mestdagh, J.-M., Visticot, J.-P.: Binding energies of first and second shell water molecules in the $Fe(H_2O)^{2+}$, $Co(H_2O)^{2+}$ and $Au(H_2O)^{2+}$ cluster ions. Eur. Phys. J. D **14**, 89–95 (2001).
254. Jayaweera, P., Blades, A. T., Ikonomou, M. G., Kebarle, P.: Production and study in the gas phase of multiply charged solvated or coordinated metal ions, J. Am. Chem. Soc. **112**, 2452–2454 (1990).
255. Stace, A. J.: Metal ion solvation in the gas phase: The quest for higher oxidation states. J. Phys. Chem. A **106**, 7993–8005 (2002).
256. Schröder, D., Schwarz, H.: Generation, stability, and reactivity of small multiply charged ions in the gas phase. J. Phys. Chem. A **103,** 7385–7394 (1999).
257. Beyer, M., Williams, E. R., V. E. Bondybey: Unimolecular reactions of dihydrated alkaline earth metal dications $M^{2+}(H_2O)_2$, M = Be, Mg, Ca, Sr, and Ba: Salt-Bridge mechanism in the proton-transfer reaction $M^{2+}(H_2O)_2 \rightarrow MOH^+ + H_3O^+$. J. Am. Chem. Soc. **121**, 1565–1573 (1999).
258. Rodriquez-Cruz, S. E., Jockusch, R. A., Williams, E. R.: Binding energies of hexahydrated alkaline earth metal ions, $M^{2+}(H_2O)_6$, M = Mg, Ca, Sr, Ba: evidence of isomeric structures for magnesium. J. Am. Chem. Soc. **121**, 1986–1987 (1999).
259. Rodriquez-Cruz, S. E., Klassen, J. S., Williams, E. R.: Hydration of gas-phase ions formed by electrospray ionization. J. Am. Soc. Mass Spectrom. **10**, 958–968 (1999).
260. Rodriquez-Cruz, S. E., Jockusch, R. A., Williams, E. R.: Hydration energies and structures of alkaline earth metal ions, $M^{2+}(H_2O)_n$, n = 5–7, M = Mg, Ca, Sr and Ba. J. Am. Chem. Soc. **121**, 8898–8906 (1999).
261. Bush, M. F., Saykally, R. J., Williams, E. R.: Formation of hydrated triply charged metal ions from aqueous solutions using nanodrop mass spectrometry. Int. J. Mass Spectrom. **253**, 256–262 (2006).
262. Shvartsburg, A. A., Siu, K. W. M.: Is there a minimum size for aqueous doubly charged metal cations? J. Am. Chem. Soc. **123**, 10071–10075 (2001).

263. Walker, N. R., Grieves, G. A., Jaeger, J. B., Walters, R. S., Duncan, M. A.: Generation of unstable doubly charged metal ion complexes in a laser vaporization cluster source. Int. J. Mass Spec. **228**, 285–295 (2003).
264. Beyer, M. K.: Hydrated metal ions in the gas phase. Mass Spectrom. Rev. **26**, 517–541 (2007).
265. Trachtman, M., Markham, G. D., Glusker, J. P., George, P., Bock, C. W.: Interactions of metal ions with water: Ab initio molecular orbital studies of structure, bonding enthalpies, vibrational frequencies and charge distributions. 1. Monohydrates. Inorg. Chem. **37**, 4421–4431 (1998).
266. Markham, G. D., Glusker, J. P., George, P., Bock, C. W.: The arrangement of first- and second-sphere water molecules in divalent magnesium complexes: Results from molecular orbital and density functional theory and from structural crystallography. J. Phys. Chem. B **106**, 5118–5134 (2002).
267. Irigoras, A., Fowler, J. E., Ugalde, J. M.: Reaction of Sc^+ and V^+ with water. J. Am. Chem. Soc. **121**, 574–580 (1999).
268. Irigoras, A., Fowler, J. E., Ugalde, J. M.: Reaction of Cr^+, Mn^+ and Fe^+ with water. J. Am. Chem. Soc. **121**, 8549–8558 (1999).
269. Irigoras, A., Elizalde, O., Silanes, I., Fowler, J. E., Ugalde, J. M.: Reactivity of $Co^+(^3F,^5F)$, $Ni^+(^2D,^4F)$, and $Cu^+(^1S,^3D)$: Reaction of Co^+, Ni^+ and Cu^+ with water. J. Am. Chem. Soc. **122**, 114–122 (2000).
270. Feller, D., Glendening, E. D., de Jong, W. A.: Structures and binding enthalpies of $M^+(H_2O)_n$ clusters, M = Cu, Ag, Au. J. Chem. Phys. **110**, 1475–1491 (1999).
271. Lee, E. C., Lee, H. M., Tarakeshwar, P., Kim, K. S.: Structures, energies and spectra of aqua-silver (I) complexes. J. Chem. Phys. **119**, 7725–7736 (2003).
272. Lee, H. M., Min, S. K., Lee, E. C., Min, J.-H., Odde, S., Kim, K. S.: Hydrated copper and gold monovalent cations: Ab initio study. J. Chem. Phys. **122**, 064314 (2005).
273. Taylor, M. S., Muntean, F., Lineberger, W. C., McCoy, A. B.: A theoretical and computational study of the anion, neutral and cation $Cu(H_2O)$ complexes. J. Chem. Phys. **121**, 5688–5699 (2004).
274. Reveles, J. U., Calaminich, P., Beltran, M. R., Köster, A. M., Khanna, S. N.: H_2O nucleation about Au^+. J. Am. Chem. Soc. **129**, 15565–15571 (2007).
275. Miliordos, E., Xantheas, S. S.: Elucidating the mechanism behind the stabilization of multi-charged metal cations in water: A case study of the electronic states of microhydrated Mg^{2+}, Ca^{2+} and Al^{3+}. Phys. Chem. Chem. Phys. **16**, 6886–6892 (2014).
276. Miliordos, E., Xantheas, S. S.: Unimolecular and hydrolysis channels for the detachment of water from microsolvated alkaline earth dication (Mg^{2+}, Ca^{2+}, Sr^{2+}, Ba^{2+}) clusters. Theor. Chem. Acc. **133**, 1450 (2014).
277. Garza-Galindo, R., Castro, M., Duncan, M. A.: Theoretical study of nascent hydration in the $Fe^+(H_2O)_n$ system. J. Phys. Chem. A **116**, 1906–1913 (2012).
278. Western, C. M.: PGOPHER: A program for simulating rotational, vibrational, and electronic spectra. J. Quant. Spectros. Rad. Trans. **186**, 221–242 (2017).
279. Carnegie, P. D., Duncan, M. A.: Water solvation shells around vanadium cations, unpublished work.
280. Muertterties, E. L., Bleeke, J. R., Wucherer, E. J., Albright, T. A.: Structural, stereochemical and electronic features of arene-metal complexes. Chem. Rev. **82**, 499–525 (1982).
281. Ma, J. C., Dougherty, D. A.: The cation-π interaction. Chem. Rev. **97**, 1303–1324 (1997).

282. Dougherty, D. A.: The cation-π interaction. Acc. Chem. Res. **46**, 885–853 (2013).
283. Mahadevi, A. S., Sastry, G. N.: Cation-π interaction: Its role and relevance in chemistry, biology, and materials science. Chem. Rev. **113**, 2100–2138 (2013).
284. Sodupe, M., Bauschlicher, C. W., Jr.: Theoretical study of the bonding of the first- and second-row transition metal positive ions to acetylene. J. Phys. Chem. **95**, 8640–8645 (1991).
285. Stockigt, D., Schwarz, J., Schwarz, H.: Theoretical and experimental studies on the bond dissociation energies of Al(methane)$^+$, Al(acetylene)$^+$, Al(ethene)$^+$, and Al(ethane)$^+$. J. Phys. Chem. **100**, 8786−8790 (1996).
286. Gidden, J., Van Koppen, P. A. M., Bowers, M. T.: Dehydrogenation of ethene by Ti^+ and V^+: Excited state effects on the mechanism for C−H bond activation from kinetic energy release distributions. J. Am. Chem. Soc. **119**, 3935−3941 (1997).
287. Sievers, M. R., Jarvis, L. M., Armentrout, P. B.: Transition metal ethene bonds: Thermochemistry of $M^+(C_2H_4)_n$ (M = Ti – Cu, n = 1 and 2) complexes. J. Am. Chem. Soc. **120**, 1891−1899 (1998).
288. Manard, M. J., Kemper, P. R., Carpenter, C. J., Bowers, M. T.: Dissociation reactions of diatomic silver cations with small alkenes: experiment and theory. Int. J. Mass. Spectrom. **241**, 99−108 (2005).
289. Sharma, P., Attah, I., Momoh, P., El-Shall, M. S.: Metal acetylene cluster ions $M^+(C_2H_2)_n$ as a model for studying reactivity of laser-generated transition metal cations. Int. J. Mass Spectrom. **300**, 81−90 (2011).
290. Meyer, F., Khan, F. A., Armentrout, P. B.: Thermochemistry of transition metal benzene complexes: Binding energies of $M(C_6H_6)_x^+$ (x = 1,2) for Ti to Cu. J. Am. Chem. Soc. **117**, 9740–9748 (1995).
291. Lin, C.-Y., Dunbar, R. C.: Radiative association kinetics and binding energies of chromium ions with benzene and benzene derivatives. Organometallics **16**, 2691–2697 (1997).
292. Li, Y., Baer, T.: Dissociation kinetics of energy-selected $(C_6H_6)Cr^+$ ions: Benzene-chromium neutral and ionic bond energies. J. Phys. Chem. A **106**, 9820–9826 (2002).
293. Willey, K. F., Cheng, P. Y., K. D. Pearce, Duncan, M. A.: Photoinitiated charge transfer and dissociation in mass-selected metalloorganic complexes. J. Phys. Chem. A **94**, 4769–4772 (1990).
294. Willey, K. F., Cheng, P. Y., M. B. Bishop, Duncan, M. A.: Charge-transfer photochemistry in ion-molecule cluster complexes of silver. J. Am. Chem. Soc. **113**, 4721–4728 (1991).
295. Willey, K. F., C. S. Yeh, Robbins, D. L., Duncan, M. A.: Charge-transfer in the photodissociation of metal ion-benzene complexes. J. Phys. Chem. **96**, 9106–9111 (1992).
296. Jaeger, T. D., Duncan, M. A.: Photodissociation of $M^+(benzene)_x$ complexes (M = Ti, V, Ni) at 355 nm. Int. J. Mass. Spectrom. **241**, 165–171 (2005).
297. Hoshino, K., Kurikawa, T., Takeda, H., Nakajima, A., Kaya, K.: Structures and ionization energies of sandwich clusters $(V_n(benzene)_m)$. J. Phys. Chem. **99**, 3053–3055 (1995).
298. Yasuike, T., Nakajima, A., Yabushita, S., Kaya, K.: Why do vanadium atoms form multiple-decker sandwich clusters with benzene molecules efficiently? J. Phys. Chem. A **101**, 5360–5367 (1997).
299. Nakajima, A., Kaya, K.: A novel network structure of organometallic clusters in the gas phase. J. Phys. Chem. A, **104**, 176–191 (2000).

300. C.W. Bauschlicher, Jr., Partridge, H., Langhoff, S. R.: Theoretical study of transition-metal ions bound to benzene. J. Phys. Chem. **96**, 3273–3278 (1992).
301. Dargel, T. K., Hertwig, R. H., Koch, W.: How do coinage metal ions bind to benzene? Mol. Phys. **96**, 583–591 (1999).
302. Yang, C. N., Klippenstein, S. J.: Theory and modeling of the binding in cationic transition metal-benzene complexes. J. Phys. Chem. **103**, 1094–1103 (1999).
303. Chaquin, P., Costa, D., Lepetit, C., Che, M.: Structure and bonding in a series of neutral and cationic transition metal-benzene η^6 complexes $[M(\eta^6\text{-}C_6H_6)]^{n+}$ (M=Ti, V, Cr, Fe, Co, Ni, and Cu). Correlation of charge transfer with the bathochromic shift of the e_1 ring vibration. J. Phys. Chem. A **105**, 4541–4545 (2001).
304. Kim, D., Hu, S., Tarakeshwar, P., Kim, K. S., Lisy, J. M.: Cation-π interactions: A theoretical investigation of the interaction of metallic and organic cations with alkenes, arenes, and heteroarenes. J. Phys. Chem. A. **107**, 1228–1238 (2003).
305. Horváthová, L., Dubecký, M., Mitas, L., Štich, I.: Spin multiplicity and symmetry breaking in vanadium-benzene complexes. Phys. Rev. Lett. **109**, 053001 (2012).
306. Horváthová, L., Dubecký, M., Mitas, L., Štich, I.: Quantum Monte Carlo study of π-bonded transition metal organometallics: Neutral and cation vanadium-benzene and cobalt-benzene half sandwiches. J. Chem. Theory Comput. **9**, 390–400 (2013).
307. Maner, J. A., Mauney, D. T., Duncan, M. A.: Imaging charge transfer in a cation-π system: velocity-map imaging of Ag^+(benzene) photodissociation. J. Phys. Chem. Lett. **6**, 4493−4498 (2015).
308. Snavely, D. L., Walters, V. A., Colson, S. D., Wiberg, K. B.: FTIR spectrum of benzene in a supersonic expansion. Chem. Phys. Lett. **103**, 423–429 (1984).
309. Reishus, N. R., Duncan, M. A.: IR spectroscopy in the fingerprint region for vanadium- and cobalt-benzene complexes, work in progress.